Electronic Supplementary Information for

Helical Polycyclic Hydrocarbons with Open-Shell Singlet Ground States and Ambipolar Redox Behaviors

Qing Jiang,*[a] Hui Tang,[a] Yuchen Peng,[a] Zhenni Hu[a] and Wangdong Zeng*[b]

[a]*College of Chemistry and Bioengineering, Hunan University of Science and Engineering, Yongzhou 425100, China.*

[b]*School of Materials Science and Engineering, Hunan University of Science and Technology, Xiangtan 411201, China.*

Email: qjiang198@163.com; wangdong.zeng@hnust.edu.cn

Table of Contents

1. Experimental Section

1.1 General

All reagents were purchased from commercial sources without further purification. Anhydrous dichloromethane (DCM) was distilled from CaH_2. Anhydrous THF was distilled from sodium-benzophenone immediately prior to use. ^1H and ^{13}C NMR spectra were recorded using 500 MHz Bruker spectrometer in $CDCl_3$, CD_2Cl_2, CD_3CN, or THF-d_8 with tetramethylsilane (TMS) as the internal standard. The chemical shift was recorded in ppm and the following abbreviations were used to explain the multiplicities: s = singlet, d = doublet, t = triplet, m = multiplet, br = broad. HR APCI mass spectra were recorded on a MicrOTOFQII instrument. UV-vis absorption was recorded on a Shimadzu UV-3600 spectrophotometer. Cyclic voltammetry measurements were performed in dry dichloromethane on a CHI 620C electrochemical analyzer with a three-electrode cell, using 0.1 M Bu_4NPF_6 as supporting electrolyte, AgCl/Ag as reference electrode, gold disk as working electrode, Pt wire as counter electrode, and scan rate at 100 mV s^{-1}. The potential was externally calibrated against the ferrocene/ferrocenium couple. The single crystal was measured at low temperature (T = 100K) on a four circles goniometer Kappa geometry Bruker AXS D8 Venture equipped with a Photon 100 CMOS active pixel sensor detector using a Copper monochromatized (= 1.54178 Å) X-Ray radiation. Continuous wave X-band ESR spectra were obtained with a Bruker ELEXSYS E500 spectrometer using a variable temperature Bruker liquid nitrogen cryostat.

1.2. Synthetic procedures and characterization data

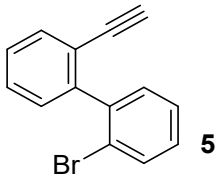

5

A mixture of THF (25 mL) and H_2O (5 mL) was sparged with N_2. After 20 min, **3** (2.82g, 10 mmol), **4** (2.18 g, 10 mmol), K_2CO_3 (2.76 g, 20 mmol) and $Pd(PPh_3)_4$ (231 mg, 0.2 mmol) were added to the flask. The reaction mixture was heated at 90 °C for 24 h under nitrogen. After cooling to room temperature, the resulting suspension was filtered and washed with diethyl ether. The combined filtrates were concentrated under reduced pressure. The resulting residue was dissolved in DCM (30 mL) and methanol (30 mL), and then K_2CO_3 (2.76 g, 20 mmol) was added. The reaction was stirred at room temperature for overnight. After that, the solvent was removed under reduced pressure and the residue was purified on a silica-gel column chromatography (hexane) to give 2.19 g of compound **5** in 86% yield as a colorless liquid. ^1H NMR ($CDCl_3$, 500 MHz): δ ppm 7.69 (dd, ^3J = 8.0 Hz, ^4J = 0.85 Hz, 1H), 7.64 (dd, ^3J = 7.75 Hz, ^4J = 1.15 Hz, 1H), 7.43 (td, ^3J = 7.55 Hz, ^4J = 1.45 Hz, 1H), 7.40-7.34 (m, 3H), 7.30 (dd, ^3J = 7.6 Hz, ^4J = 1.05 Hz, 1H), 7.27-7.25 (m, 1H), 2.97 (s, 1H); ^{13}C NMR ($CDCl_3$, 125 MHz) δ ppm 144.2, 141.5, 133.1, 132.8, 131.4, 129.9, 129.3, 128.6, 127.9, 127.1, 123.5, 121.9, 82.3, 80.6; HR-MS (APCI): calcd for $C_{14}H_9Br$ $(M+H)^+$: 256.9960; found, 256.9961 (error: 0.39 ppm).

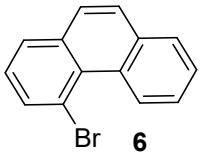

6

The flask was charged with **5** (2.09 g, 8.2 mmol), $PtCl_2$ (100 mg, 0.37 mmol) and dry DCE (20 mL) under nitrogen atmosphere. The mixture was stirred at 80 °C for 12 h. After cooling to room temperature, the solvent was removed under reduced pressure and the residue was purified by column chromatography (hexane) to give compound **6** (82%, 1.71 g) as a colorless solid. ^{1}H NMR ($CDCl_3$, 500 MHz): δ ppm 10.06 (d, J = 7.95 Hz, 1H), 8.00 (dd, ^3J = 7.6 Hz, ^4J = 1.25 Hz, 1H), 7.90 (dd, ^3J = 7.35 Hz, ^4J = 1.45 Hz, 1H), 7.84 (dd, ^3J = 7.8 Hz, ^4J = 1.0 Hz, 1H), 7.75 (d, J = 8.7 Hz, 1H), 7.70-7.63 (m, 3H), 7.38 (t, J = 7.7 Hz, 1H); ^{13}C NMR ($CDCl_3$, 125 MHz) δ ppm 135.4, 134.9, 133.6, 130.0, 129.1, 128.8, 128.7, 128.4, 127.4, 127.2, 126.9, 126.8, 125.6, 119.8; HR-MS (APCI): calcd for $C_{14}H_9Br$ $(M)^+$: 256.9982; found, 255.9885 (error: 1.17 ppm).

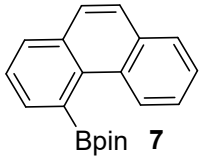

7

To an oven dried flask was added **6** (1.5 g, 5.9 mmol), $B(pin)_2$ (2.54 g, 10 mmol), $Pd(dppf)Cl_2$ (73 mg, 0.1 mmol), KOAc (1.76 g, 18 mmol) and dioxane (50 mL). The reaction mixture was heated at 90 °C for 15 h under nitrogen. After cooling to room temperature, the resulting suspension was filtered and washed with diethyl ether. The combined filtrates were concentrated under reduced pressure and purified on a silica-gel column chromatography (hexane/CH_2Cl_2 = 4:1, v/v) to give 1.36 g of compound **7** in 76% yield as a colorless solid. ^{1}H NMR ($CDCl_3$, 500 MHz): δ ppm 8.57 (d, J = 7.8 Hz, 1H), 7.93 (dd, ^3J = 7.85 Hz, ^4J = 1.1 Hz, 1H), 7.90 (dd, ^3J = 7.35 Hz, ^4J = 1.45 Hz, 1H), 7.85 (dd, ^3J = 6.85 Hz, ^4J = 1.0 Hz, 1H), 7.76-7.71 (m, 2H), 7.62-7.55 (m, 3H), 1.51 (s, 12H); ^{13}C NMR ($CDCl_3$, 125 MHz) δ ppm 134.0, 133.1, 133.0, 132.5, 131.1, 130.7, 128.5, 127.7, 127.1, 126.72, 126.71, 125.8, 125.3, 84.5, 25.0 (one sp^2 carbon signal was not observed because of overlapping); HR-MS (APCI): caldc for $C_{20}H_{21}BO_2$ $(M)^+$: 304.1629; found, 304.1630 (error: 0.33 ppm).

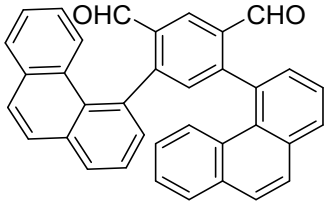

9

A mixture of THF (15 mL) and H_2O (3 mL) was sparged with N_2. After 20 min, **7** (0.46 g, 1.5 mmol), 2,4-dibromobenzene-1,3-dicarboxaldehyde **8** (145 mg, 0.5 mmol), K_2CO_3 (0.35 g, 2.5 mmol) and $Pd(PPh_3)_4$ (50 mg, 0.04 mmol) were added to the flask. The reaction mixture was heated at 90 °C for 48 h under nitrogen. After cooling to room temperature, the resulting suspension was filtered

and washed with diethyl ether. The combined filtrates were concentrated under reduced pressure and purified on a silica-gel column chromatography (hexane/CH_2Cl_2 = 3:1, v/v) to give 0.194 g of two rotamers **9** (the ratio of two rotamers is 1:1.06) in 80% yield as a yellow solid. ^{1}H NMR ($CDCl_3$, 500 MHz): δ ppm 9.84 (s, 2H), 9.76 (s, 2H), 8.89 (s, 1H), 8.85 (s, 1H), 8.11 (d, *J* = 8.95 Hz, 2H), 7.99 (dd, ^3J = 3.85 Hz, ^4J = 1.45 Hz, 2H), 7.97 (dd, ^3J = 3.85 Hz, ^4J = 1.4 Hz, 2H), 7.89 (d, *J* = 1.1 Hz, 1H), 7.88 (d, *J* = 1.7 Hz, 2H), 7.86 (d, *J* = 1.2 Hz, 1H), 7.79-7.78 (m, 8H), 7.72 (s, 1H), 7.67 (s, 1H), 7.66 (s, 1H), 7.65-7.60 (m, 5H), 7.53-7.51 (m, 2H), 7.50-7.48 (m, 2H), 7.46 (d, *J* = 1.4 Hz, 1H), 7.45 (d, *J* = 1.4 Hz, 2H), 7.43 (d, *J* = 1.4 Hz, 1H), 7.41 (td, ^3J = 7.75 Hz, ^4J = 1.5 Hz, 2H), 7.28 (td, ^3J = 7.5 Hz, ^4J = 1.45 Hz, 2H); ^{13}C NMR ($CDCl_3$, 125 MHz) δ ppm 190.9, 190.8, 154.1, 153.9, 134.4, 134.2, 133.93, 133.92, 133.73, 133.72, 133.71, 133.4, 133.3, 131.7, 131.4, 130.4, 129.7, 129.6, 129.4, 129.2, 129.0, 128.7, 128.6, 128.53, 128.52, 127.8, 127.6, 127.4, 126.8, 126.13, 126.12, 125.92, 125.91 (five sp2 carbon signals were not observed because of overlapping); HR-MS (APCI): caldc for $C_{32}H_{22}O_2$ $(M+H)^+$:487.1693; found, 487.1703 (error: 2.05 ppm).

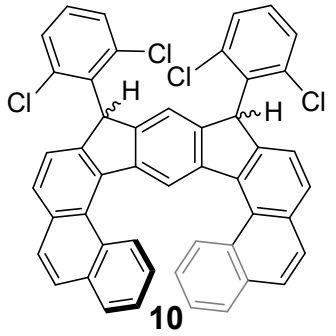

10

To an oven dried flask was added THF (20 mL) and 2.6-dichloro-1-bromobenzene (0.475 g, 2.1 mmol). The mixture was cooled to 0 °C and isopropylmagnesium chloride (2.0 M, 1 mL) was added slowly. The reaction was stirred for 2 h and then the compound **9** (100 mg, 0.2 mmol) was added in one portion. The mixture was warmed to room temperature overnight. The reaction was quenched with saturated NH_4Cl solution and the organic phase was washed with water and then brine solution. The organic layer was dried over Na_2SO_4 and the volatiles removed. The crude product was then dissolved in 50 mL dry DCM under nitrogen atmosphere and 0.5 mL of $BF_3{\cdot}OEt_2$ was added. The mixture was stirred for 30 minutes and quenched by methanol. The solvent was removed under reduced pressure and then purified on a silica-gel column chromatography (hexane/CH_2Cl_2 = 8:1, v/v) to give 0.131 g of two isomers **10** (the ratio of two isomers is 1:0.12) in 88% yield as a colorless solid. ^{1}H NMR ($CDCl_3$, 500 MHz): δ ppm 9.99 (s, 1H), 8.58 (d, *J* = 8.3 Hz, 2H), 7.89 (dd, ^3J = 8.0 Hz, ^4J = 0.75 Hz, 2H), 7.80-7.75 (m, 4H), 7.73 (d, *J* = 7.85 Hz, 2H), 7.54 (dd, ^3J = 8.05 Hz, ^3J = 1.4 Hz, 2H), 7.37-7.32 (m, 4H), 7.23 (t, *J* = 8.0 Hz, 2H), 7.17 (dd, ^3J= 7.85 Hz, ^4J = 1.35 Hz, 2H), 7.09 (s, 1H), 6.57 (td, ^3J = 7.7 Hz, ^4J = 1.15 Hz 2H), 6.27 (s, 2H); ^{13}C NMR ($CDCl_3$, 125 MHz) δ ppm 147.4, 146.7, 141.6, 137.8 ,137.6, 137.1, 136.2, 133.1, 133.0, 130.2, 129.1, 128.4, 128.3, 127.5, 127.4, 127.3, 127.0, 126.7, 124.0, 122.2, 118.8, 118.0, 51.3; HR-MS (APCI): caldc for $C_{48}H_{26}Cl_4$ $(M+H)^+$:743.0861; found, 743.0865 (error: 0.54 ppm).

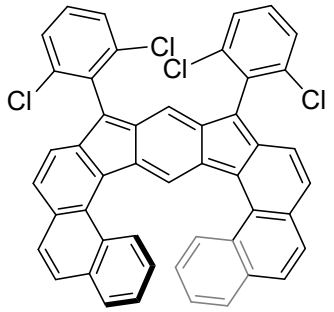

H1

Under argon atmosphere and in the dark, a 50 ml flask containing a magnetic stir bar was charged with **10** (50 mg, 0.067 mmol), tetrabutoxide potassium (34 mg, 0.3 mmol), 18-crown-6 (79 mg, 0.3 mmol) and THF (20 mL). The resulting mixture was stirred at room temperature for 12 h, then *p*-chloranil (49 mg, 0.2 mmol) was added, and the mixture was continued stirred for 30 min. Then the solvent was removed under reduced pressure at room temperature and the resulting residue was directly subjected to flash chromatography (silica gel was neutralized with Et_3N, DCM/Hexane = 1:3). Black solid **H1** was obtained in 87% yield (43 mg). ^{1}H NMR (THF-d_8, 500 MHz, -20 ^{o}C): δ ppm 7.93 (d, *J* = 8.3 Hz, 2H), 7.62 (s, 1H), 7.56 (d, *J* = 8.35 Hz, 2H), 7.47 (d, *J* = 8.15 Hz, 4H), 7.42 (d, *J* = 8.55 Hz, 2H), 7.33 (t, *J* = 8.125 Hz, 2H), 7.10 (t, *J* = 7.45 Hz, 2H), 7.07 (d, *J* = 8.6 Hz, 2H), 6.43 (d, *J* = 8.6 Hz, 2H), 6.38 (t, *J* = 7.5 Hz, 2H), 5.85 (d, *J* = 8.5 Hz, 2H), 5.45 (s, 1H); HR-MS analysis (APCI): calcd for $C_{48}H_{24}Cl_4$ $(M+H)^+$: 741.0705; found, 741.0687 (error: 2.4 ppm).

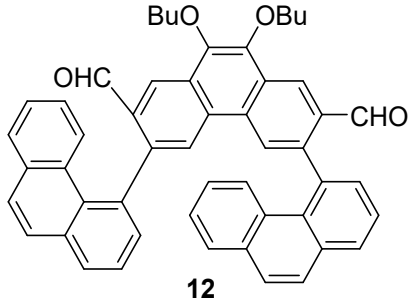

12

A mixture of THF (15 mL) and H_2O (3 mL) was sparged with N_2. After 20 min, **7** (0.304 g, 1.0 mmol), **11** (160 mg, 0.3 mmol), K_2CO_3 (0.35 g, 2.5 mmol) and $Pd(PPh_3)_4$ (50 mg, 0.043 mmol) were added to the flask. The reaction mixture was heated at 90 ^{o}C for 48 h under nitrogen. After cooling to room temperature, the resulting suspension was filtered and washed with diethyl ether. The combined filtrates were concentrated under reduced pressure and purified on a silica-gel column chromatography (hexane/CH_2Cl_2 = 3:1, v/v) to give 0.184 g of two rotamers **12** (the ratio of two rotamers is 2:1) in 84% yield as a yellow solid. ^{1}H NMR ($CDCl_3$, 500 MHz): δ ppm 9.73 (s, 2H), 9.72 (s, 1H), 9.08 (d, *J* = 5.25 Hz, 3H), 8.69 (d, *J* = 0.8 Hz, 3H), 7.97 (d, *J* = 7.15 Hz, 3H), 7.84 (d, *J* = 7.4 Hz, 2H), 7.82-7.77 (m, 5H), 7.74 (t, *J* = 10.4 Hz, 2H), 7.63 (t, *J* = 7.25 Hz, 1H), 7.60-7.55 (m, 3H), 7.52-7.48 (m, 3H), 7.47-7.45 (m, 2H), 7.41 (t, *J* = 7.45 Hz, 2H), 7.34 (t, *J* = 7.43 Hz, 1H), 7.03-7.01 (m, 3H), 4.55- 4.50 (m, 2H), 4.48-4.43 (m, 2H), 4.42-4.37 (m, 2H), 2.09-2.03 (m, 6H), 1.77-1.69 (m, 6H), 1.13-1.10 (m, 9H); ^{13}C NMR ($CDCl_3$, 125 MHz) δ ppm 191.9, 191.8, 144.83,

144.82, 144.52, 144.51, 135.7, 135.6, 133.84, 133.83, 133.6, 133.3, 132.3, 132.1, 130.9, 130.1, 130.0, 129.63, 129.62, 129.2, 129.1, 128.3, 127.7, 127.6, 127.4, 127.3, 126.5, 126.1, 126.0, 125.9, 125.8, 124.0, 123.9, 74.1, 32.8, 19.8, 14.3(eleven sp^2 carbon signals and four sp^3 carbon signals were not observed because of overlapping); HR-MS (APCI): caldc for $C_{52}H_{42}O_2$ $(M+H)^+$: 731.3105; found, 731.3113 (error: 1.07 ppm).

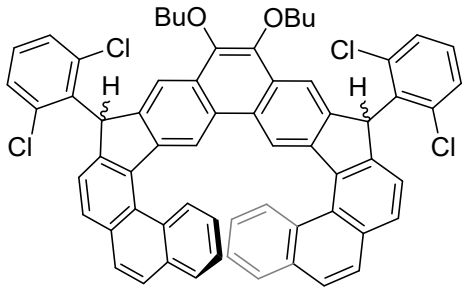

13

To an oven dried flask was added THF (20 mL) and 2.6-dichloro-1-bromobenzene (0.475 g, 2.1 mmol). The mixture was cooled to 0 °C and isopropylmagnesium chloride (2.0 M, 1 mL) was added slowly. The reaction was stirred for 2 h and then the compound **12** (100 mg, 0.14 mmol) was added in one portion. The mixture was warmed to room temperature overnight. The reaction was quenched with saturated NH_4Cl solution and the organic phase was washed with water and then brine solution. The organic layer was dried over Na_2SO_4 and the volatiles removed. The crude product was then dissolved in 50 mL dry DCM under nitrogen atmosphere and 0.5 mL of $BF_3{\cdot}OEt_2$ was added. The mixture was stirred for 30 minutes and quenched by methanol. The solvent was removed under reduced pressure and then purified on a silica-gel column chromatography (hexane/CH_2Cl_2 = 3:1, v/v) to give 0.124 g of two isomers **13** (the ratio of two isomers is 2:1) in 90% yield as a pale yellow solid. ^{1}H NMR ($CDCl_3$, 500 MHz): δ ppm 9.82 (s, 1H), 9.80 (s, 2H), 9.16 (t, *J* = 8.5 Hz, 3H), 8.15 (d, *J* = 1.1 Hz, 1H), 8.10 (d, *J* = 1.2 Hz, 2H), 7.90-7.79 (m, 12H), 7.62-7.59 (m, 3H), 7.47 (d, *J* = 7.8 Hz, 1H), 7.42 (d, *J* = 7.3 Hz, 2H), 7.25 (d, *J* = 5.3 Hz, 2H),7.23 (s, 1H), 7.17-7.13 (m, 3H), 7.03-6.98 (m, 3H), 6.80-6.75 (m, 3H), 6.49 (s, 2H), 6.42 (s, 1H), 4.21-4.18 (m, 6H), 1.81-1.73 (m, 6H), 1.54-1.42 (m, 6H), 0.94-0.89 (m, 9H); ^{13}C NMR ($CDCl_3$, 125 MHz) δ ppm 148.1, 146.8, 145.3, 145.2, 143.6, 141.7, 141.5, 137.9, 137.8, 137.5, 137.2, 136.93, 136.92, 136.3, 136.2, 133.2, 133.1, 132.9, 132.8, 130.33, 130.32, 129.5, 129.3, 129.1, 128.9, 128.6, 128.54, 128.53, 128.3, 128.23, 128.22, 128.12. 128.11, 128.0, 127.9, 127.4, 127.13, 127.12, 126.9, 123.93, 123.92, 122.5, 122.2, 117.8, 117.7, 117.1, 73.7, 51.4, 51.1, 32.6, 19.7, 14.13, 14.12 (four sp^2 carbon signals and three sp^3 carbon signals were not observed because of overlapping); HR-MS (APCI): caldc for $C_{64}H_{46}Cl_4O_2$ $(M+H)^+$: 987.2324; found, 987.2328 (error: 0.40 ppm).

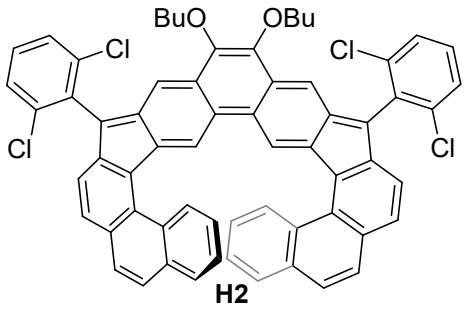

Under argon atmosphere and in the dark, a 50 ml flask containing a magnetic stir bar was charged with **13** (50 mg, 0.053 mmol), tetrabutoxide potassium (19 mg, 0.26 mmol), 18-crown-6 (69 mg, 0.26 mmol) and THF (20 mL). The resulting mixture was stirred at room temperature for12 h, then *p*-chloranil (37 mg, 0.15 mmol) was added, and the mixture was continued stirred for 30 min. Then the solvent was removed under reduced pressure at room temperature and the resulting residue was directly subjected to flash chromatography (silica gel was neutralized with Et_3N, DCM/Hexane = 1:3). Black solid **H2** was obtained in 85% yield (44 mg). The well-fined ^{1}H NMR spectra cannot be obtained due to its open-shell diradical character; HR-MS analysis (APCI): calcd for $C_{64}H_{45}Cl_4O_2$ $(M+H)^+$: 985.2168; found, 985.2152 (error: 1.60 ppm).

1.3. Chemical titration

Typical oxidation procedure to radical cation and dication: NO•SbF_6 (1 equiv. for radical cation, 2 equiv. for dication) dissolved in acetonitrile (50 μl) was added into the dry DCM solution of **H1** or **H2**. The oxidized compounds were in situ generated in 5 mins without further purification.

Typical reduction procedure to radical anion and dianion: The freshly prepared sodium anthracenide solution (0.1 M in dry THF, 1 equiv. for radical anion, 2 equiv. for dianion) was added dropwise to dry THF solution of **H1** or **H2**. The reduced compounds were in situ formed in 5 mins without further purification.

Typical deprotonation procedure to dianion: The flask was charged with to **10/13** (1 equiv.), ^{t}BuOK (5 equiv.), 18-crown-6 (5 equiv.) and dry THF. The reaction completed within 30 min, giving the corresponding dianions without further purification.

H2^{2+}: ^{1}H NMR (CD_2Cl_2, 500 MHz): δ ppm 8.75 (d, *J* = 8.05 Hz, 2H), 8.37 (s, 2H), 8.12 (d, *J* = 8.45 Hz, 2H), 7.80 (d, *J* = 7.5 Hz, 2H), 7.65-7.58 (m, 6H), 7.43 (d, *J* = 8.5 Hz, 2H), 7.30 (s, 2H), 7.17 (d, *J* = 8.55 Hz, 2H), 7.14 (t, *J* = 7.65 Hz, 2H), 7.10 (t, *J* = 7.12 Hz, 2H), 6.95 (t, *J* = 8.5 Hz, 2H), 4.09 (t, *J* = 6.35 Hz, 4H), 1.66-1.60 (m, 4H), 1.32-1.25 (m, 4H), 0.85 (t, *J* = 7.45 Hz, 6H).

H1^{2-}: ^{1}H NMR (THF-d_8, 500 MHz): δ ppm 10.42 (s, 1H), 10.23 (d, *J* = 7.8 Hz, 1H), 10.17 (d, *J* = 8.05 Hz, 1H), 8.91 (d, *J* = 8.15 Hz, 1H), 7.83 (d, *J* = 7.9 Hz, 1H), 7.68-7.66 (m, 2H), 7.57 (d, *J* = 8.3 Hz, 1H), 7.47 (d, *J* = 7.95 Hz, 2H), 7.41 (t, *J* = 7.37 Hz, 1H), 7.34 (d, *J* = 8.0 Hz, 2H), 7.29-7.17 (m, 7H), 7.08 (t, *J* = 7.4 Hz, 1H), 6.78 (d, *J* = 7.35 Hz, 1H), 6.69 (d, *J* = 7.6 Hz, 1H), 6.32 (t, *J* = 7.5 Hz, 1H).

H2^{2-}: ^{1}H NMR (THF-d_8, 500 MHz): δ ppm 10.17 (s, 2H), 9.87 (d, *J* = 8.45 Hz, 2H), 7.92 (s, 2H), 7.72 (d, *J* = 7.85 Hz, 2H), 7.64 (d, *J* = 8.3 Hz, 2H), 7.43 (d, *J* = 8.0 Hz, 4H), 7.38 (d, *J* = 8.3 Hz,

2H), 7.29 (d, J = 8.35 Hz, 2H), 7.27 (d, J = 8.45 Hz, 2H), 7.05 (t, J = 8.0 Hz, 2H), 6.93 (t, J = 7.27 Hz, 2H), 6.67 (t, J = 7.57 Hz, 2H), 4.25 (t, J = 6.15 Hz, 4H), 1.91-1.85 (m, 4H), 1.71-1.65 (m, 4H), 1.02 (t, J = 7.3 Hz, 6H).

2. Additional spectra

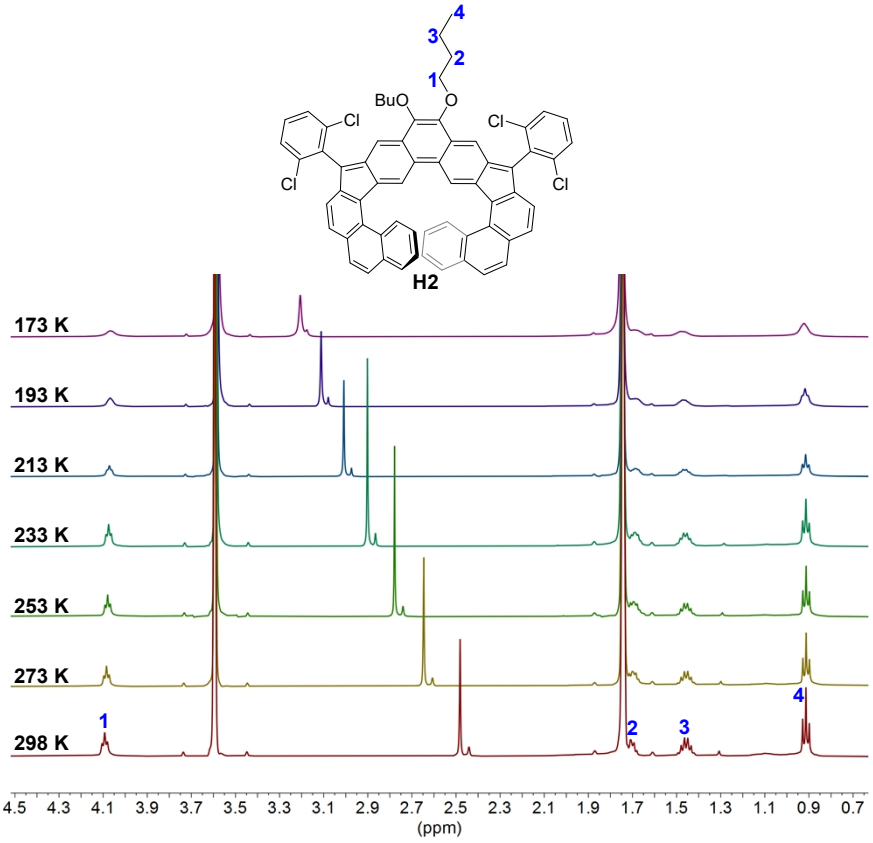

Figure S1. VT ^{1}H NMR spectra (aliphatic region) of **H2** in THF-d_8.

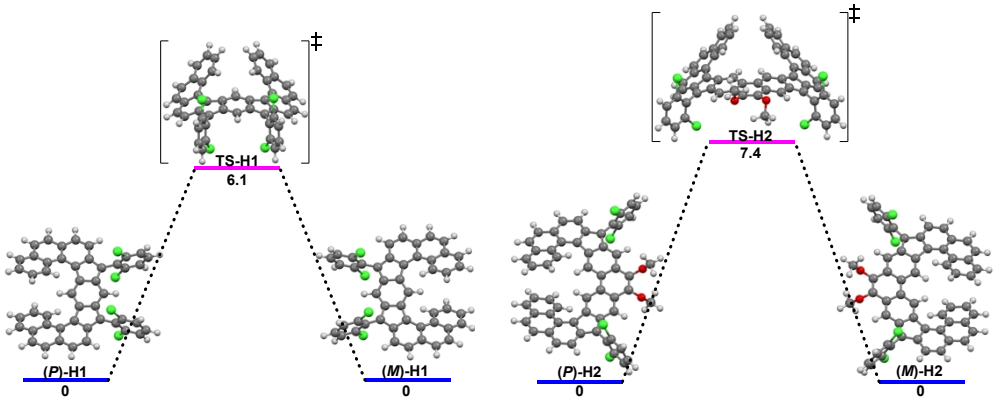

Figure S2. Racemization between *P*-isomer and *M*-isomer of **H1** and **H2**. The relative Gibbs free energy (unit: kcal/mol) was calculated at the B3LYP/6-311G(d) level.

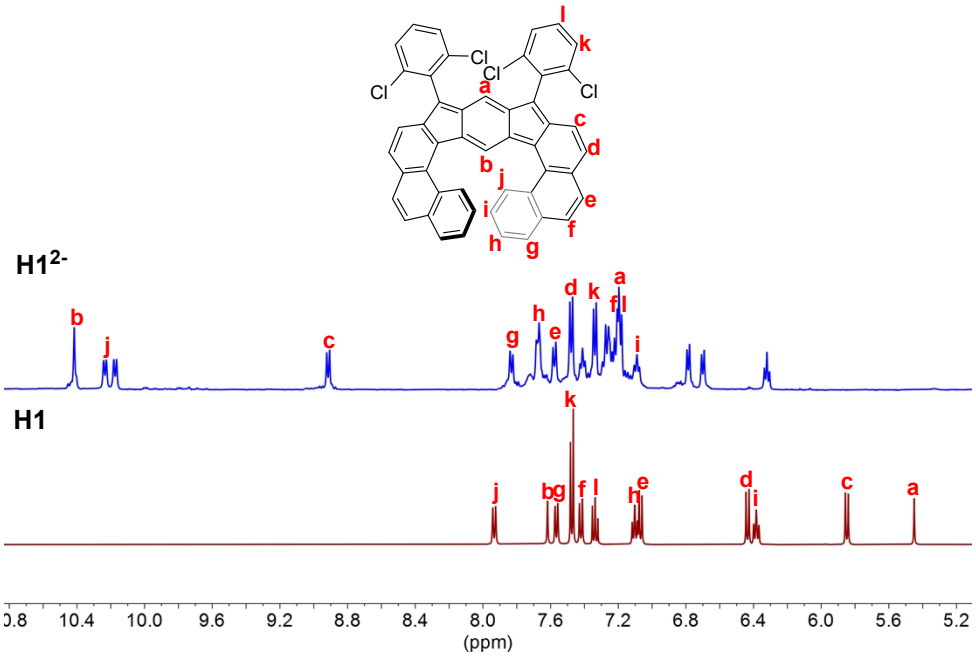

Figure S3. ^{1}H NMR spectra (aromatic region) of **H1** (in[D_8]THF) and **H1**$^{2-}$ (in [D_8]THF).

3. DFT calculations

Theoretical calculations were performed with the Gaussian09 rev. D program suite.[1] All calculations were carried out using the density functional theory (DFT) method with Becke's three-parameter hybrid exchange functionals and the Lee-Yang-Parr correlation functional (B3LYP) employing the 6-31G(d,p) basis set for all atoms.[2] Natural orbital occupation number (NOON)) calculations were done by spin unrestricted LC-BLYP/6-31G(d) method and the diradical character (y_0) was calculated according to Yamaguchi's scheme: $y_0 = 1 - (2T/(1 + T^2))$, and $T = (n_{HONO} - n_{LUNO})/2$ (n_{HONO} is the occupation number of the HONO, n_{LUNO} is the occupation number of the LUNO).[3] Time-dependent DFT (TD-DFT) calculations have been performed at the B3LYP/6-31G(d,p) level of theory. NICS values were calculated using the standard GIAO procedure.[4] AICD plot was calculated by using the method developed by Herges.[5] Electrostatic potential maps and Hirshfeld charge were calculated at the B3LYP/6-31G(d,p).

In the study of racemization processes, molecular geometries of all stationary points were optimized at the B3LYP level of DFT with the 6-31G(d) basis set with IEPCM model as solvation of THF at 298 K. Harmonic vibration frequency calculations at the same level were performed to verify all stationary points as local minima (with no imaginary frequency) or transition states (with one imaginary frequency). Frequency analyses were also used to evaluate the zero-point vibrational energy and thermal corrections at 298 K. IRC calculations[6] were also performed to check transition states.

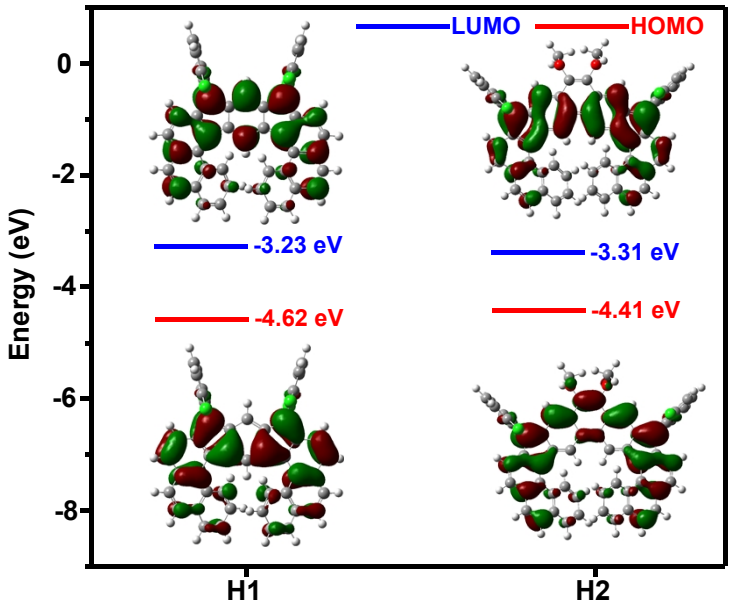

Figure S4. Calculated (RB3LYP/6-31g(d,p)) HOMO and LUMO profiles of **H1** and **H2**.

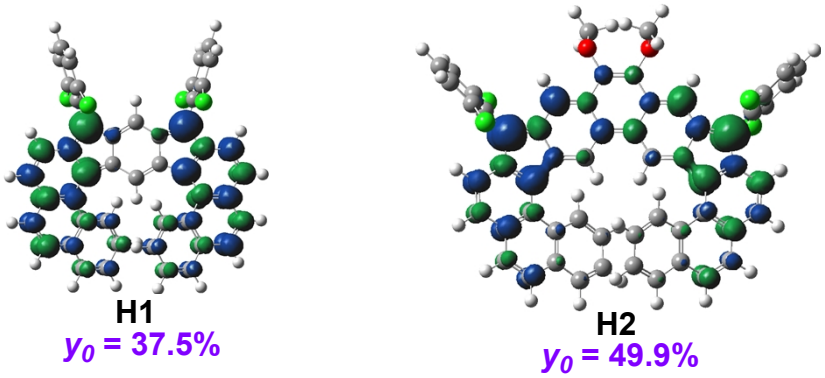

Figure S5. Calculated spin-density distribution (LC-UBLYP/6-31G(d,p)) of the singlet ground states of **H1** and **H2**$^-$, and their calculated diradical character (y_0). Blue and green surfaces represent ***α*** and ***β*** spin density, respectively.

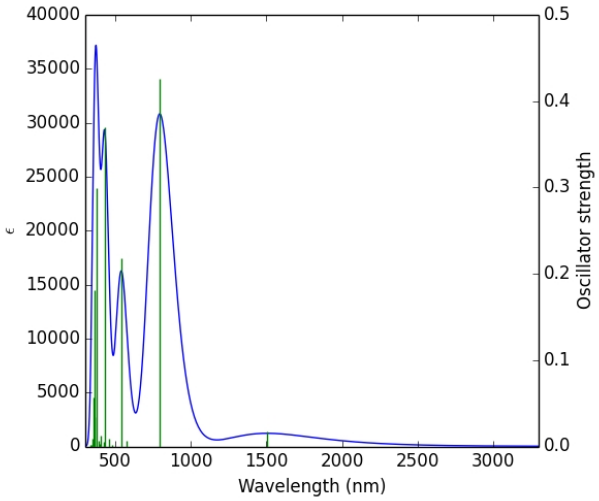

Figure S6. TD DFT simulated spectra of **H1.**

Table S1. Selected TD-DFT (RB3LYP/6-31G(d,p)) calculated energies, oscillator strength and compositions of major electronic transitions of **H1**. H=HOMO, L=LUMO, L+1=LUMO+1, etc.

Wavelength (nm)	Osc. Strength (*f*)	Major contributions
1504.1	0.0168	H-1->L (21%), H->L (79%)
794.4	0.4254	H-1->L (77%), H->L (22%)
539.8	0.2186	H-3->L (62%), H-2->L (36%)
432.1	0.3699	H-4->L (12%), H->L+1 (77%), H-5->L (3%)
380.0	0.2994	H-1->L+1 (73%), H->L+3 (18%)
362.7	0.1813	H-1->L+1 (17%), H->L+3 (78%)
355.3	0.0562	H-1->L+2 (12%), H->L+4 (74%), H->L+5 (10%)

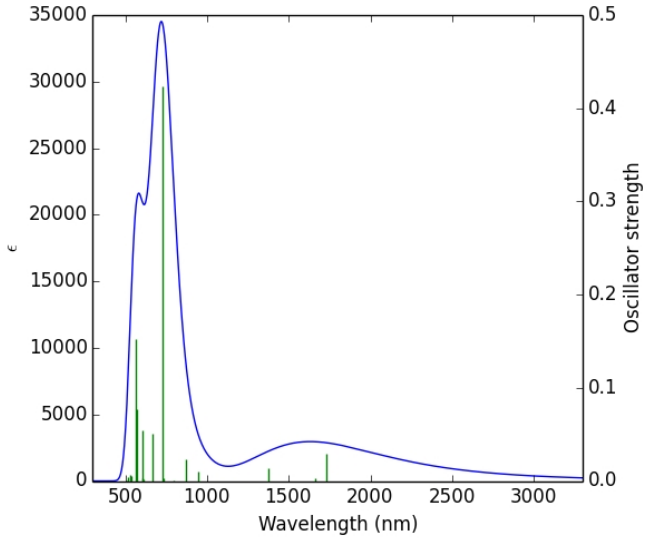

Figure S7. TD DFT simulated spectra of **H1**$^{\cdot+}$**.**

Table S2. Selected TD-DFT (UB3LYP/6-31G(d,p)) calculated energies, oscillator strength and compositions of major electronic transitions of **H1**$^{\cdot+}$. H=HOMO, L=LUMO, L+1=LUMO+1, etc.

Wavelength (nm)	Osc. Strength (*f*)	Major contributions
1733.3	0.0297	H (A)->L (A) (85%), H-1(A)->L (A) (3%), H (B)->L+1(B) (9%)
1659.3	0.003	H (B)->L (B) (97%)
1377.9	0.0137	H-1(A)->L (A) (82%), H (B)->L+1(B) (15%)
870.2	0.0229	H-1(B)->L (B) (94%), H-4(A)->L (A) (2%)
728.0	0.424	H-2(B)->L (B) (46%), H (B)->L+1(B) (35%)
608.3	0.0544	H-6(B)->L (B) (45%), H-4(B)->L (B) (19%), H-1(B)->L+1(B) (20%)
573.0	0.0776	H-4(B)->L(B) (61%), H-1(B)->L+1(B) (10%), H-3(A)->(A) (3%)
567.4	0.1523	H-6(B)->L (B) (34%), H-4(B)->L (B) (10%), H-2(B)->L+1(B) (15%), H-1(B)->L+1(B) (20%)

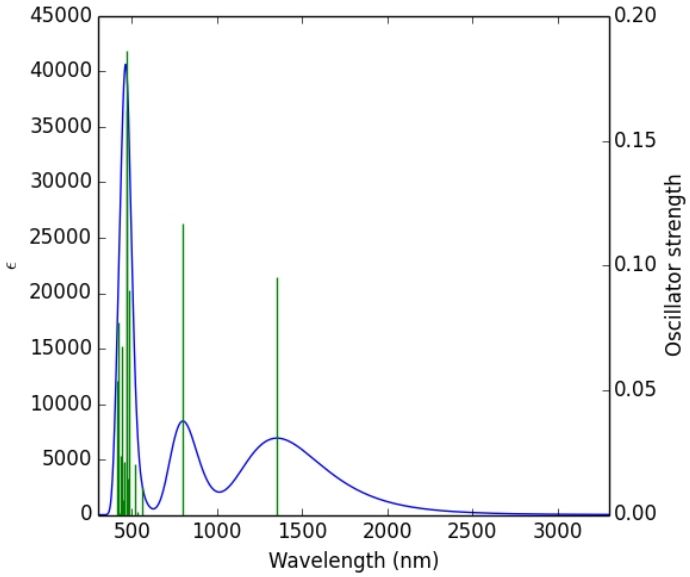

Figure S8. TD DFT simulated spectra of **H1**$^{\cdot-}$**.**

Table S3. Selected TD-DFT (UB3LYP/6-31G(d,p)) calculated energies, oscillator strength and compositions of major electronic transitions of **H1**$^{\cdot-}$. H=HOMO, L=LUMO, L+1=LUMO+1, etc.

Wavelength (nm)	Osc. Strength (*f*)	Major contributions
1352.5	0.0954	H (B)->L (B) (96%) H-1(B)->L (B) (2%)
799.8	0.1167	H-1(B)->L(B) (94%), H(B)->L (B) (2%)
559.9	0.0112	H-1(A)->L(A) (37%), H(B)->L+1(B) (43%), H (A)->L+1(A) (8%)
515.7	0.0204	H (A)->L+1(A) (67%), H (B)->L+1(B) (17%), H-

		2(A)->L+2(A) (2%), H-4(B)->L(B) (4%), H(B)->L+3(B) (3%)
481.3	0.0903	H(A)->L+3(A) (67%), H-2(A)->L (A) (4%), H-1(A)->L (A) (4%), H-1(A)->L+2(A) (2%), H (A)->L+1(A) (4%), H (A)->L+6(A) (2%), H-1(B)->L+1(B) (5%), H (B)->L+3(B) (3%)
469.2	0.186	H (A)->L+2(A) (43%), H (A)->L+7(A) (15%), H-3(B)->L (B) (21%) H-2(B)->L (B) (3%), H (B)->L+2(B) (6%), H (B)->L+4(B) (5%)
468.1	0.1622	H-1(A)->L (A) (38%), H (B)->L+1(B) (31%), H-2(A)->LUMO(A) (2%), H-1(A)->L+2(A) (2%), H (A)->L+1(A) (2%), H(A)->L+3(A) (9%), H (A)->L+6(A) (2%), H-1(B)->L+1(B) (5%), H (B)->L+3(B) (7%)
422.3	0.0773	H-1(A)->L+1(A) (63%), H (B)->L+4(B) (16%), H (A)->L+2(A) (3%), H-3(B)->L (B) (2%), H-1(B)->L+2(B) (4%), H (B)->L+2(B) (4%)

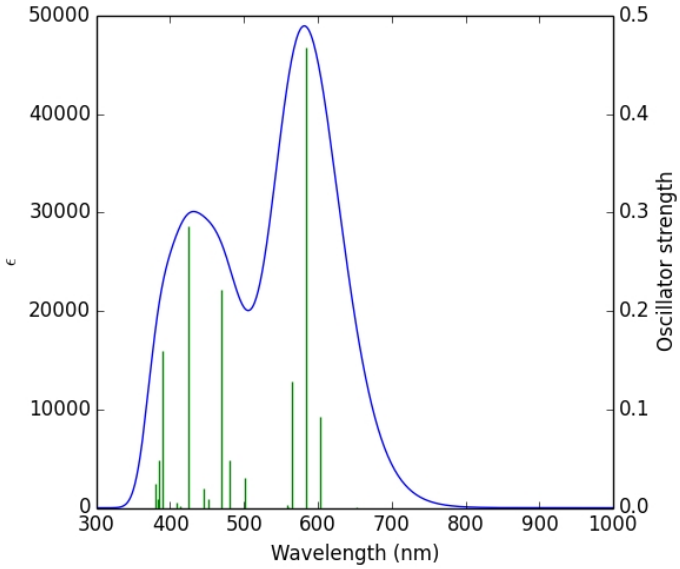

Figure S9. TD DFT simulated spectra of $\mathbf{H1^{2-}}$

Table S4. Selected TD-DFT (RB3LYP/6-31G(d,p)) calculated energies, oscillator strength and compositions of major electronic transitions of $\mathbf{H1^{2-}}$. H=HOMO, L=LUMO, L+1=LUMO+1, etc.

Wavelength (nm)	Osc. Strength (*f*)	Major contributions
652.0	0.0003	H->L (98%)
603.2	0.0926	H->L+1 (92%), H-1->L (3%), H->L+3 (4%)
583.8	0.468	H->L+2 (97%)

564.1	0.1281	H->L+3 (94%), H->L+1 (4%)
469.9	0.2216	H-1->L (89%), H-1->L+2 (3%), H->L+1 (2%)
424.7	0.2862	H-1->L+3 (90%), H-1->L+1 (3%), H->L+10 (2%)
389.5	0.1594	H-2->L (89%), H-2->L+2 (3%), H->L+11 (2%)

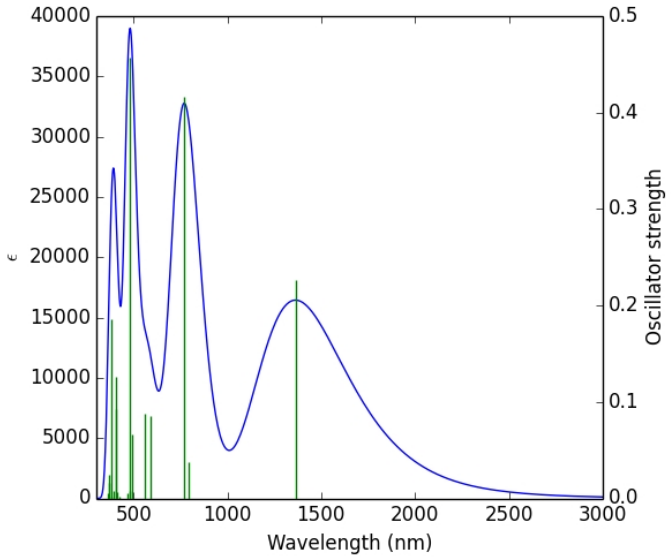

Figure S10. TD DFT simulated spectra of **H2.**

Table S5. Selected TD-DFT (RB3LYP/6-31G(d,p)) calculated energies, oscillator strength and compositions of major electronic transitions of **H2**. H=HOMO, L=LUMO, L+1=LUMO+1, etc.

Wavelength (nm)	**Osc. Strength (*f*)**	**Major contributions**
1362.6	0.2269	H-1->L (11%), H->L (92%)
768.2	0.4161	H-1->L (86%), H->L (10%), H-3->L (3%)
560.1	0.0882	H-4->L (96%)
479.3	0.0226	H->L+1 (91%), H-3->L (3%)
404.7	0.1261	H-10->L (70%), H->L+3 (27%)
382.2	0.1854	H->L+4 (83%), H-11->L (2%), H-9->L (2%), H->L+6 (7%)
366.6	0.0242	H-13->L (83%), H-1->L+2 (7%), H->L+5 (3%)

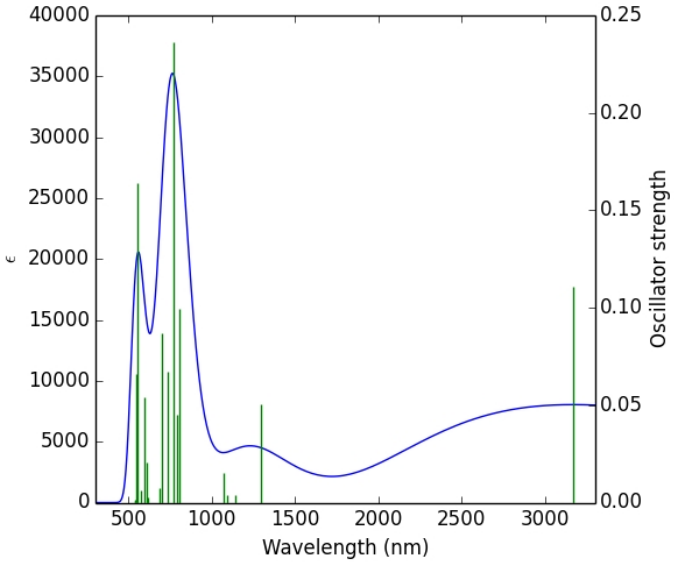

Figure S11. TD DFT simulated spectra of **H2**$^{\cdot+}$**.**

Table S6. Selected TD-DFT (UB3LYP/6-31G(d,p)) calculated energies, oscillator strength and compositions of major electronic transitions of **H2**$^{\cdot+}$. H=HOMO, L=LUMO, L+1=LUMO+1, etc.

Wavelength (nm)	Osc. Strength (*f*)	Major contributions
3170.1	0.1109	H (A)->L (A) (96%), H (B)->L+1(B) (2%)
1295.0	0.0502	H-1(A)->L (A) (79%), H (B)->L+1(B) (15%)
804.1	0.0997	H-4(A)->L (A) (28%), H-2(B)->L (B) (30%), H-1(B)->L+1(B) (30%)
772.2	0.2364	H-1(A)->L (A) (10%), H-1(B)->L (B), (16%), H (B)->L+1(B) (56%), H-3(A)->L (A) (9%)
698.2	0.0872	H-4(A)->L (A) (14%), H-2(B)->L(B) (59%), H-1(B)->L+1(B) (20%)
550.8	0.1642	H-5(B)->L (B) (75%), H-3(A)->L (A) (2%), H-10(B)->L+1(B) (3%), H-7(B)->L (B) (2%), H-4(B)->L+1(B) (5%)
548.1	0.0661	H-4(B)->L (B) (14%), H-3(B)->L+1(B) (69%)

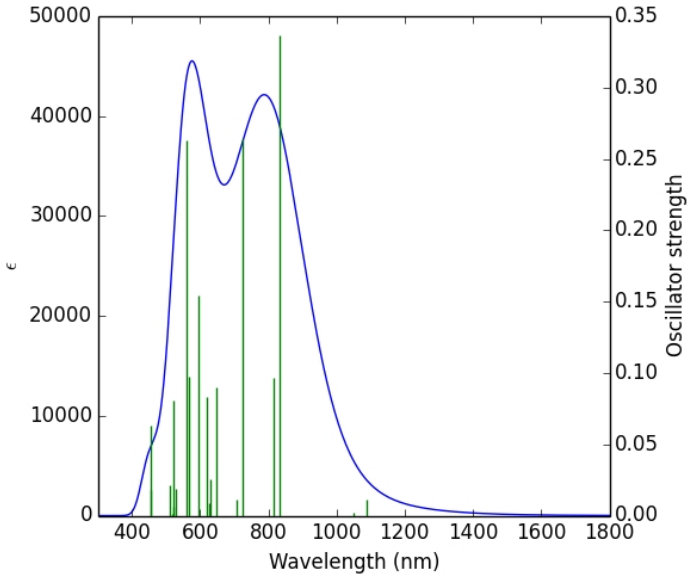

Figure S12. TD DFT simulated spectra of **H2**$^{2+}$**.**

Table S7. Selected TD-DFT (RB3LYP/6-31G(d,p)) calculated energies, oscillator strength and compositions of major electronic transitions of **H2**$^{2+}$. H=HOMO, L=LUMO, L+1=LUMO+1, etc.

Wavelength (nm)	Osc. Strength (*f*)	Major contributions
1088.8	0.0112	H->L (86%), H-2->L (3%), H-1->L+1 (9%)
834.2	0.3366	H-1->L (34%), H->L+1 (62%), H-2->L+1 (3%)
725.5	0.264	H-2->L (87%) H-3->L+1 (7%), H->L (5%)
593.3	0.1545	H-4->L (32%), H-3->L+1 (59%), H-2->L (3%)
558.5	0.2627	H-8->L (34%), H-7->L (22%), H-4->L+1 (33%), H-9->L+1 (7%)
521.1	0.0805	H-8->L (48%), H-4->L+1 (29%), H-9->L+1 (8%), H-7->L (8%)
453.1	0.0633	H-10->L (63%), H-8->L+1 (22%)

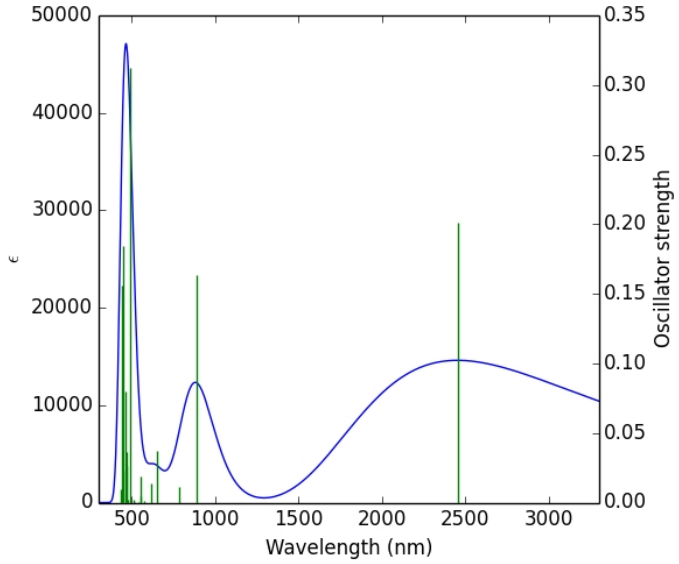

Figure S13. TD DFT simulated spectra of **H2**$^{\cdot-}$.

Table S8. Selected TD-DFT (UB3LYP/6-31G(d,p)) calculated energies, oscillator strength and compositions of major electronic transitions of **H2**$^{\cdot-}$. H=HOMO, L=LUMO, L+1=LUMO+1, etc.

Wavelength (nm)	Osc. Strength (*f*)	Major contributions
2452.7	0.2015	H (B)->L (B) (97%)
886.0	0.1637	H-1(B)->L (B) (96%)
648.8	0.037	H-1(A)->L (A) (20%), H (A)->L+1(A) (14%), H (B)->L+1(B) (54%), H-3(B)->L (B) (3%)
492.9	0.3123	H-1(A)->L (A) (42%), H (A)->L+1(A) (11%), H (A)->L+2(A) (12%) H-2(A)->L (A) (2%), H-1(A)->L+3(A) (2%), H-5(B)->L (B) (9%), H-1(B)->L+1(B) (3%), H (B)->L+1(B) (8%), H (B)->L+4(B) (3%)
462.7	0.0799	H-1(A)->L+1(A) (18%), H (A)->L+3(A) (34%), H (B)->L+5(B) (15%) H-1(A)->L+4(A) (6%), HOMO(A)->L+7(A) (5%), H-6(B)->L(B) (5%), H(B)->L+2(B) (2%), H(B)->L+3(B) (6%)
451.8	0.1844	H (A)->L+2(A) (27%), H (A)->L+4(A) (27%), H-2(A)->L (A) (6%), H-1(A)->L (A) (8%), H-1(A)->L+7(A) (4%), H-1(B)->L+1(B) (7%), H (B)->L+4(B) (7%)
445.2	0.1556	H (A)->L+3(A) (27%), H-6(B)->L (B) (43%), H (B)->L+5(B) (20%), H (B)->L+3(B) (4%)

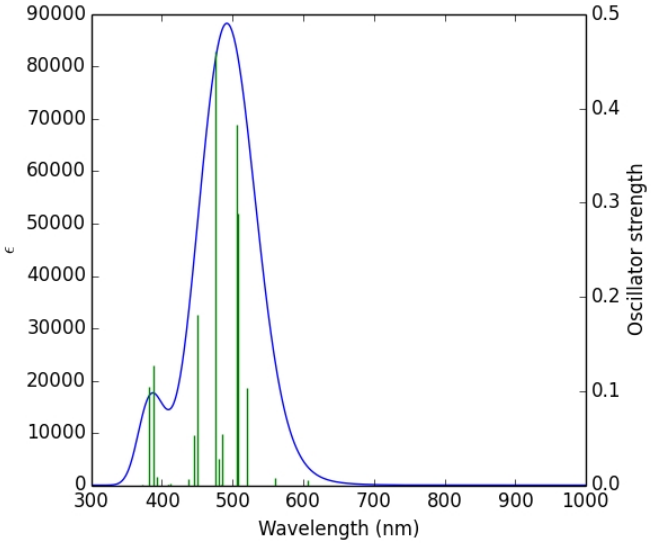

Figure S14. TD DFT simulated spectra of **$H2^{2-}$.**

Table S9. Selected TD-DFT (RB3LYP/6-31G(d,p)) calculated energies, oscillator strength and compositions of major electronic transitions of **$H2^{2-}$**. H=HOMO, L=LUMO, L+1=LUMO+1, etc.

Wavelength (nm)	Osc. Strength (*f*)	Major contributions
606.7	0.0048	H->L (97%)
520.8	0.1037	H-1->L (24%), H->L+1 (10%), H->L+2 (62%)
508.3	0.2884	H-1->L (49%), H->L+1 (16%), H->L+2 (31%)
506.1	0.383	H->L+3 (94%), H-1->L+2 (3%)
475.5	0.4605	H->L+4 (18%), H->L+6 (70%), H-1->L+3 (4%)
449.7	0.1812	H-1->L+2 (85%), H->L+7 (10%), H->L+3 (3%)
388.1	0.127	H-2->L (67%), H-1->L+7 (23%), H-3->L+1 (3%)

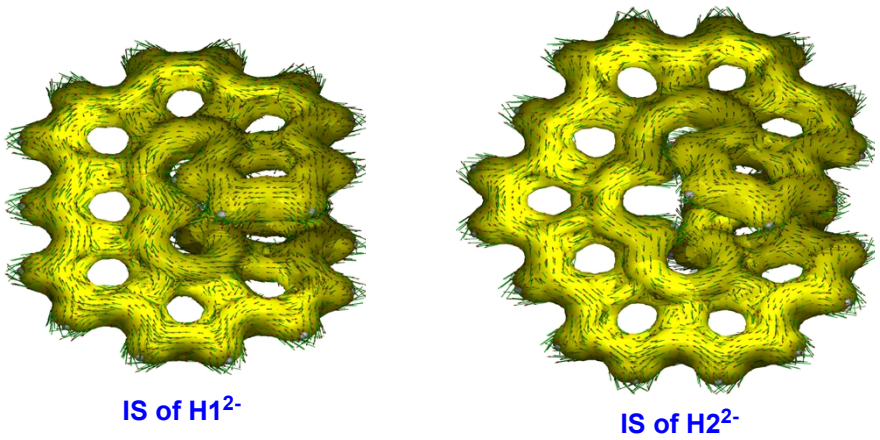

Figure S15. ACID plots of all-benzenoid expanded helicene analogues. IS = isoelectronic structure.

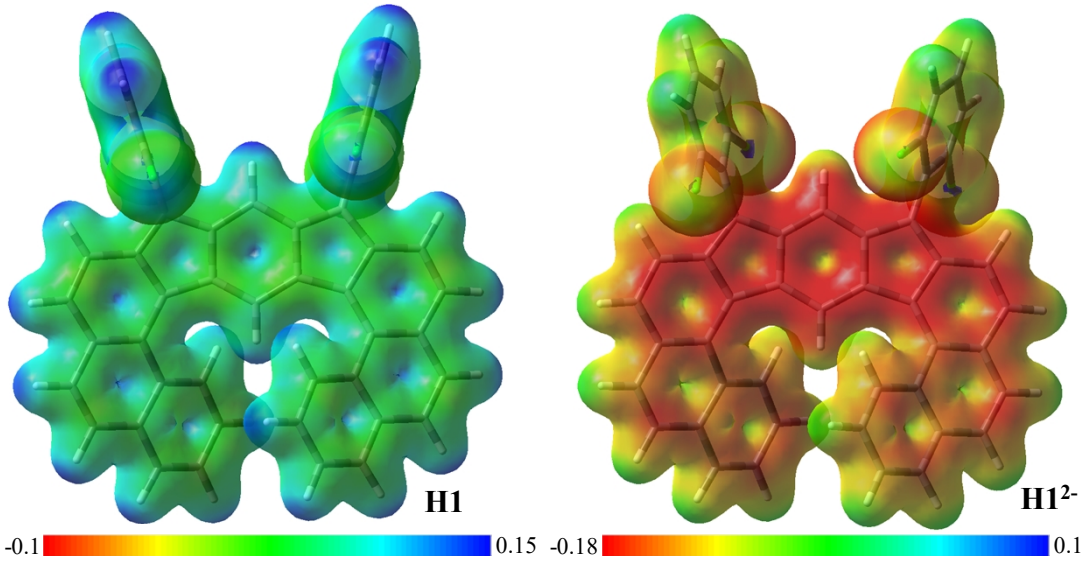

Figure S16. Calculated electrostatic potential maps for the compound **H1** and its charged species. Red regions represent more negative charges, and blue regions represent more positive charges.

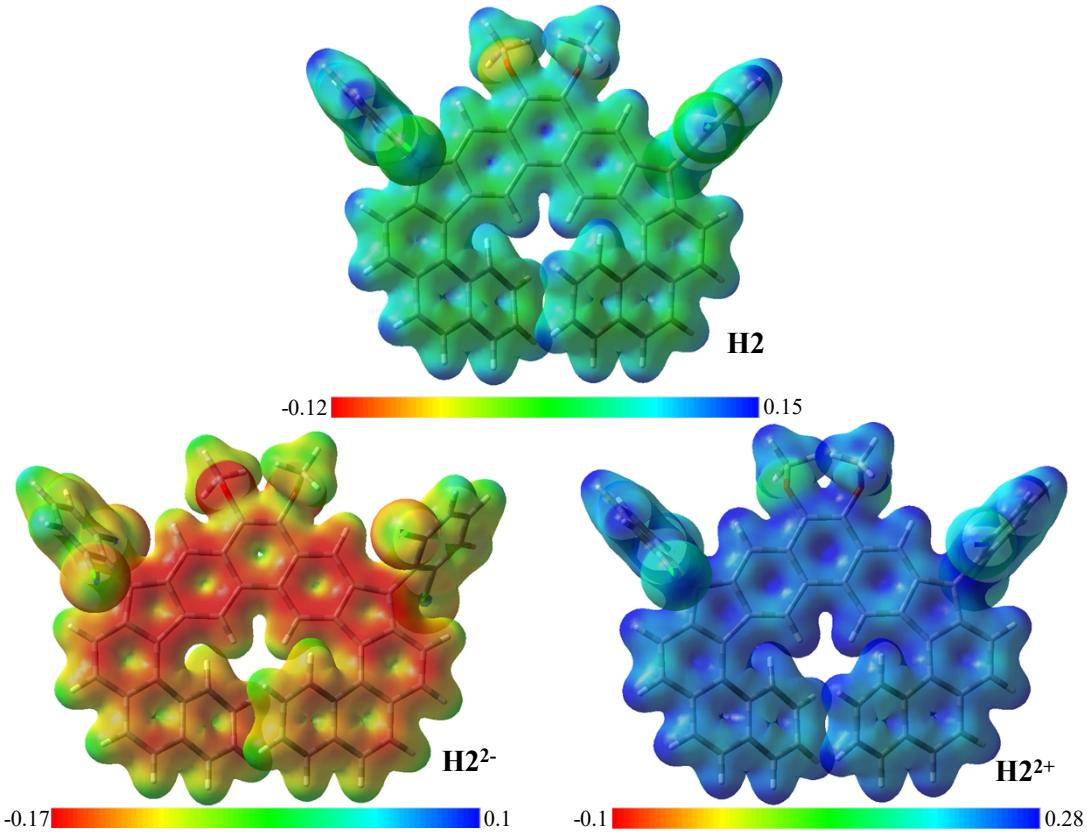

Figure S17. Calculated electrostatic potential maps for the compound **H2** and its charged species. Red regions represent more negative charges, and blue regions represent more positive charges.

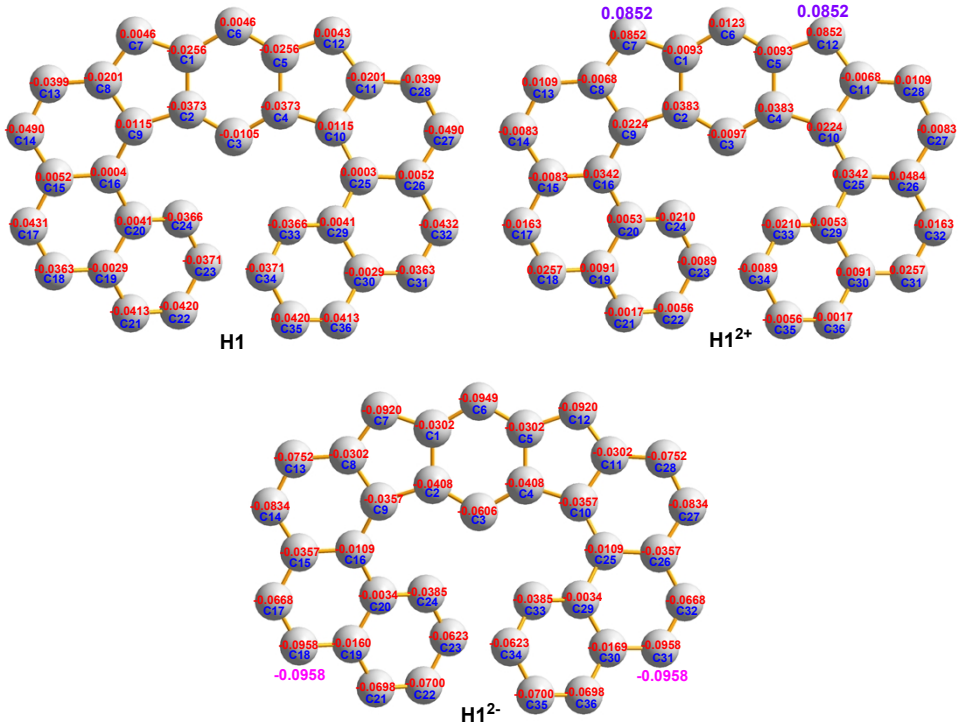

Figure S18. Hirshfeld charge distribution of **H1** and its charged species.

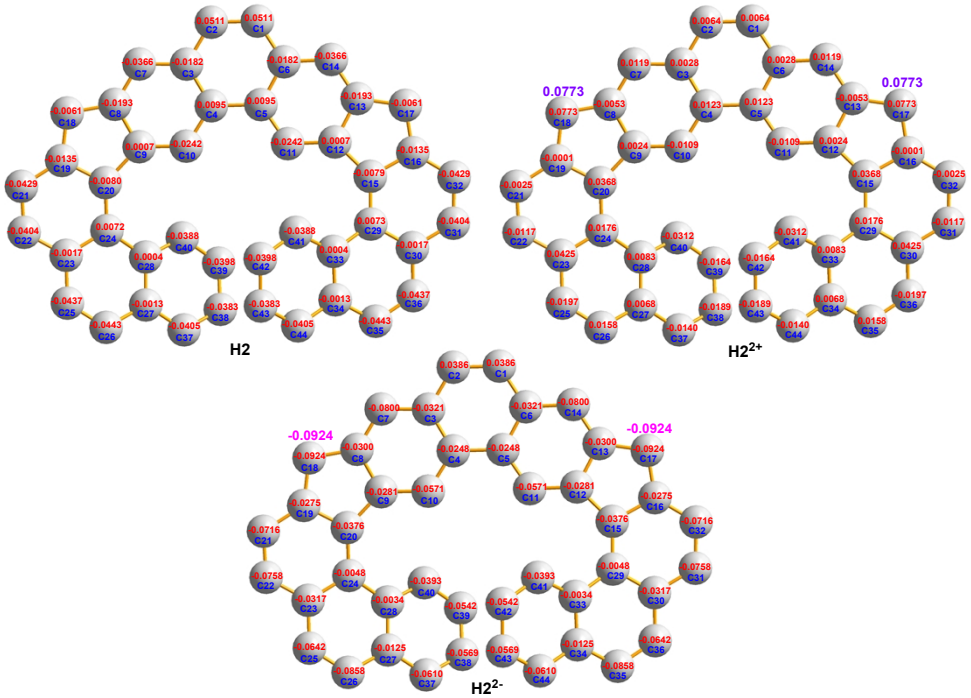

Figure S19. Hirshfeld charge distribution of **H2** and its charged species.

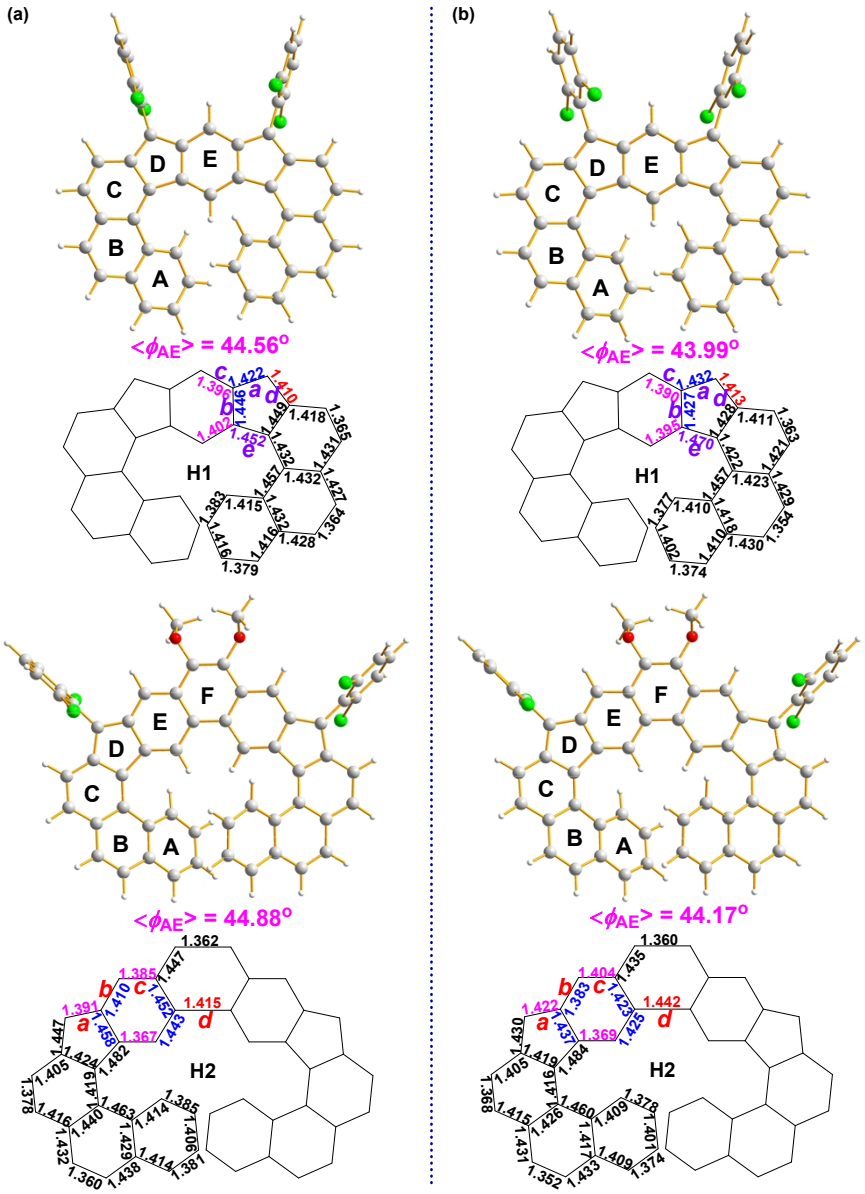

Figure S20. (a) Optimized (B3LYP/6-31G(d,p)) structures of **H1**/**H2** and selected bond lengths (in Å). (b) Optimized (CAM-B3LYP/6-31G(d,p)) structures of **H1**/**H2** and selected bond lengths (in Å). *A comparison of the torsion angle along the helical inner rim shows that the structural distortion (<Φ_{AE}> = 43.99 and 44.17° for **H1** and **H2**, respectively) at the CAM-B3LYP/6-31G(d,p) level of theory is slightly small compared to that (<Φ_{AE}> = 44.56 and 44.88° for **H1** and **H2**, respectively) at the B3LYP/6-31G(d,p) level of theory. In **H1**, the bonds a and e at the CAM-B3LYP/6-31G(d,p) level of theory are significantly longer than those at the B3LYP/6-31G(d,p) level of theory, while the bonds b and c are shortened. In **H2**, a comparison of selected bonds of optimized structures at the B3LYP/6-31G(d,p) and CAM-B3LYP/6-31G(d,p) level of theory indicates that the bonds a, c and d at the CAM-B3LYP/6-31G(d,p) level of theory are much longer, while the bond b becomes shorter.*

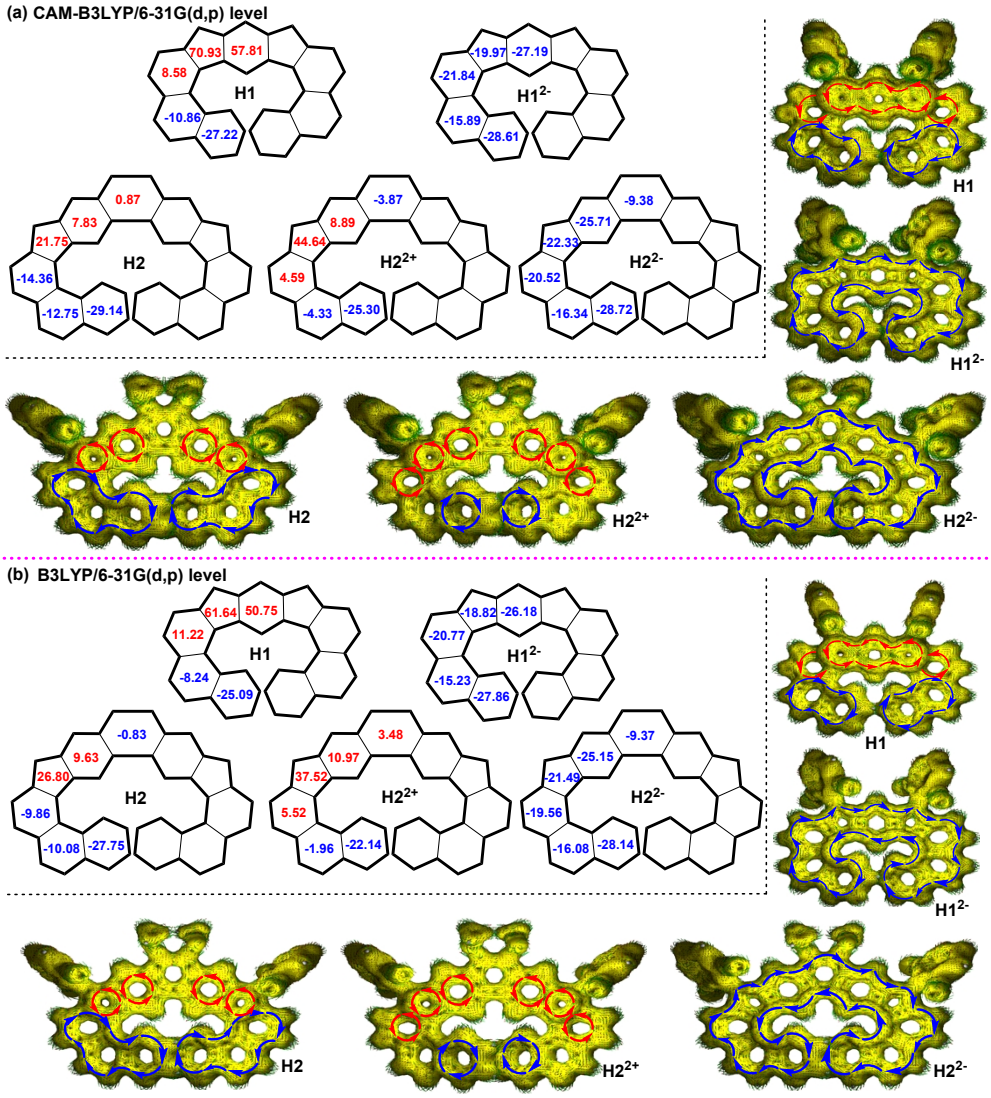

Figure S21. Calculated NICS(1)zz values (the numbers in the rings) and calculated ACID plots of H1/H2 and their charged species at the CAM-B3LYP/6-31G(d,p) (a) and B3LYP/6-31G(d,p) (b) levels of theory, respectively. The red and blue arrows indicate the counterclockwise (paratropic) and clockwise (diatropic) current flow, respectively.

4. Crystallographic data

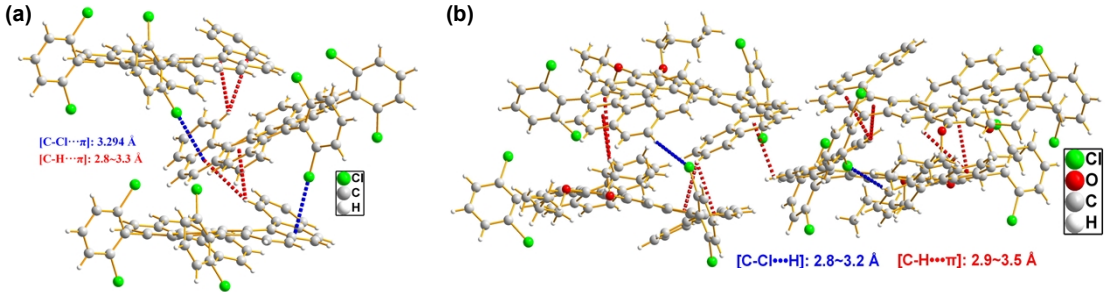

Figure S22. The crystal packing structures of **H1** (a) and **H2** (b).

Table S10. Crystal data and structure refinement for **H1.**

Identification code	JQ13O3
Empirical formula	$C_{48}H_{24}Cl_4$
Formula weight	742.47
Temperature/K	100.03
Crystal system	orthorhombic
Space group	Pbcn
a/Å	30.8986(17)
b/Å	10.7331(6)
c/Å	22.0999(13)
α/°	90
β/°	90
γ/°	90
Volume/Å^3	7329.2(7)
Z	8
ρ_{calc}g/cm^3	1.346
μ/mm^{-1}	3.197
F(000)	3040.0
Crystal size/mm^3	0.652 × 0.17 × 0.07
Radiation	CuKα (λ = 1.54178)

2Θ range for data collection/°	5.72 to 133.83
Index ranges	$-36 \leq h \leq 24, -12 \leq k \leq 12, -25 \leq l \leq 26$
Reflections collected	46283
Independent reflections	6202 [R_{int} = 0.1510, R_{sigma} = 0.0914]
Data/restraints/parameters	6202/0/469
Goodness-of-fit on F^2	1.182
Final R indexes [I>=2σ (I)]	R_1 = 0.1051, wR_2 = 0.2838
Final R indexes [all data]	R_1 = 0.1275, wR_2 = 0.3090
Largest diff. peak/hole / e $Å^{-3}$	0.78/-0.72

Table S11. Crystal data and structure refinement for **H2.**

Identification code	JQ006_0u
Empirical formula	$C_{128}H_{88}Cl_{7.96}O_4$
Formula weight	1972.21
Temperature/K	99.99
Crystal system	orthorhombic
Space group	Pbca
a/Å	29.1132(16)
b/Å	11.2694(6)
c/Å	57.979(3)
α/°	90
β/°	90
γ/°	90
Volume/$Å^3$	19022.2(18)
Z	8
ρ_{calc}g/cm^3	1.377
μ/mm^{-1}	2.627
F(000)	8187.0

Crystal size/mm^3	0.999 × 0.158 × 0.104
Radiation	CuKα (λ = 1.54178)
2Θ range for data collection/°	6.072 to 144.608
Index ranges	-35 ≤ h ≤ 35, -13 ≤ k ≤ 9, -71 ≤ l ≤ 71
Reflections collected	197228
Independent reflections	18671 [R_{int} = 0.0635, R_{sigma} = 0.0279]
Data/restraints/parameters	18671/0/1266
Goodness-of-fit on F^2	1.031
Final R indexes [I>=2σ (I)]	R_1 = 0.0436, wR_2 = 0.1117
Final R indexes [all data]	R_1 = 0.0473, wR_2 = 0.1165
Largest diff. peak/hole / e Å^{-3}	0.52/-0.30

Table S12. Crystal data and structure refinement for **$H2^{2+}$.**

Identification code	JQ
Empirical formula	$C_{64}H_{44}Cl_{17.98}O_2Sb_2$
Formula weight	1725.88
Temperature/K	106.00
Crystal system	monoclinic
Space group	C2/c
a/Å	22.6813(11)
b/Å	16.1611(11)
c/Å	19.3896(12)
α/°	90.00
β/°	108.576(4)
γ/°	90.00
Volume/Å^3	6737.1(7)
Z	4

ρ_{calc}g/cm^3	1.702
μ/mm^{-1}	13.275
F(000)	3407.0
Crystal size/mm^3	0.098 × 0.056 × 0.041
Radiation	CuKα (λ = 1.54178)
2Θ range for data collection/°	6.84 to 133.26
Index ranges	-26 ≤ h ≤ 26, -19 ≤ k ≤ 19, -23 ≤ l ≤ 22
Reflections collected	35329
Independent reflections	5944 [R_{int} = 0.0460, R_{sigma} = 0.0313]
Data/restraints/parameters	5944/177/541
Goodness-of-fit on F^2	1.084
Final R indexes [I>=2σ (I)]	R_1 = 0.0331, wR_2 = 0.0743
Final R indexes [all data]	R_1 = 0.0401, wR_2 = 0.0798
Largest diff. peak/hole / e Å^{-3}	0.81/-0.62

Table S13. Crystal data and structure refinement for **$H2^{2-}$.**

Identification code	JQ1
Empirical formula	$C_{104}H_{124}Cl_4K_2O_{18}$
Formula weight	1882.02
Temperature/K	100.00
Crystal system	triclinic
Space group	P-1
a/Å	15.9841(7)
b/Å	17.7180(8)
c/Å	23.9712(10)
α/°	92.321(3)
β/°	107.956(3)

γ/°	112.455(2)
Volume/Å^3	5871.0(5)
Z	2
ρ_{calc}g/cm^3	1.065
μ/mm^{-1}	1.998
F(000)	1996.0
Crystal size/mm^3	0.175 × 0.124 × 0.105
Radiation	CuKα (λ = 1.54178)
2Θ range for data collection/°	5.486 to 133.188
Index ranges	-19 ≤ h ≤ 18, -20 ≤ k ≤ 20, -26 ≤ l ≤ 28
Reflections collected	85059
Independent reflections	20004 [R_{int} = 0.0704, R_{sigma} = 0.0599]
Data/restraints/parameters	20004/143/1158
Goodness-of-fit on F^2	1.041
Final R indexes [I>=2σ (I)]	R_1 = 0.0961, wR_2 = 0.2608
Final R indexes [all data]	R_1 = 0.1146, wR_2 = 0.2762
Largest diff. peak/hole / e Å^{-3}	1.05/-1.24

5. NMR spectra

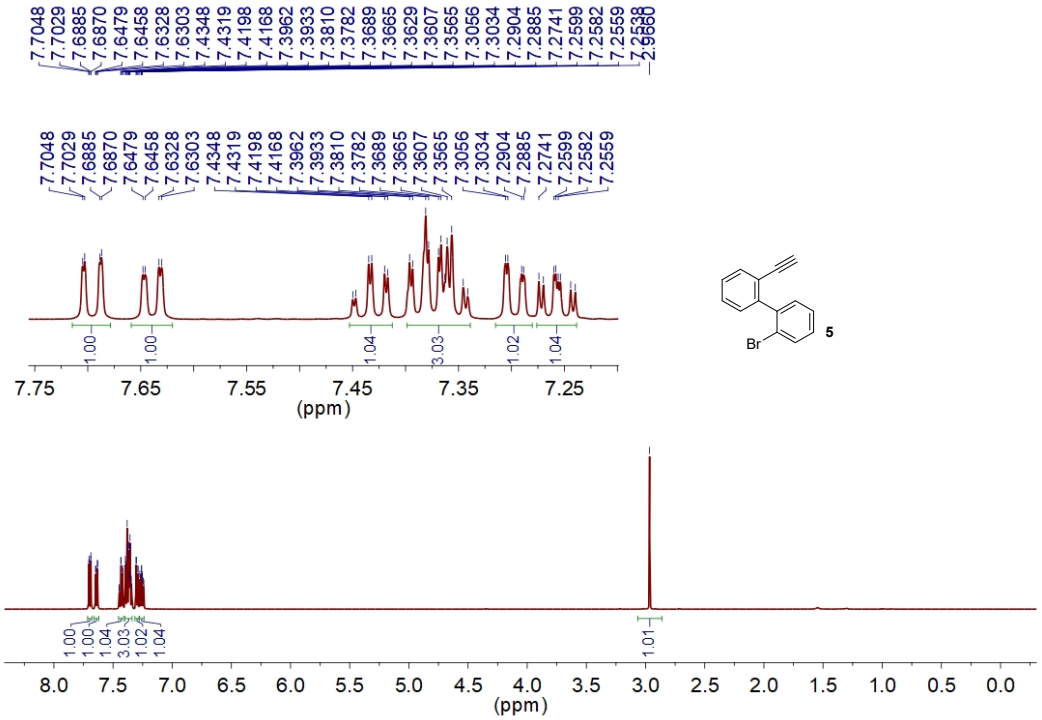

Figure S23. ^{1}H NMR (500 MHz) spectra of **5** recorded in $CDCl_3$ at room temperature.

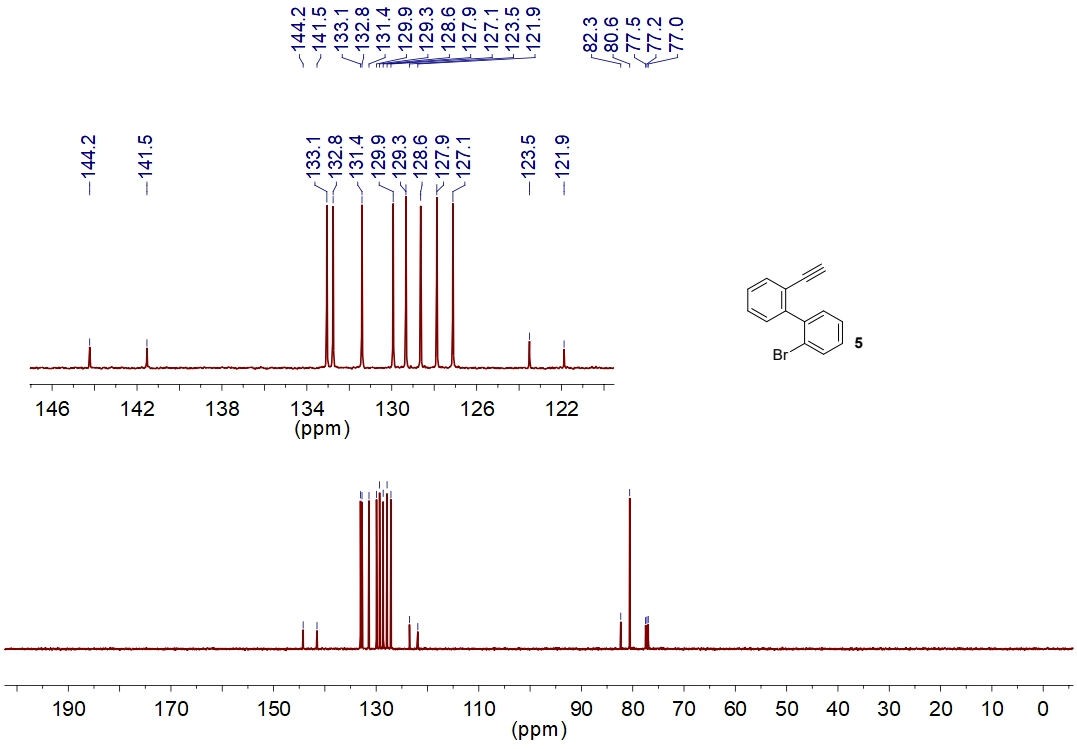

Figure S24. ^{13}C NMR (125 MHz) spectra of **5** recorded in $CDCl_3$ at room temperature.

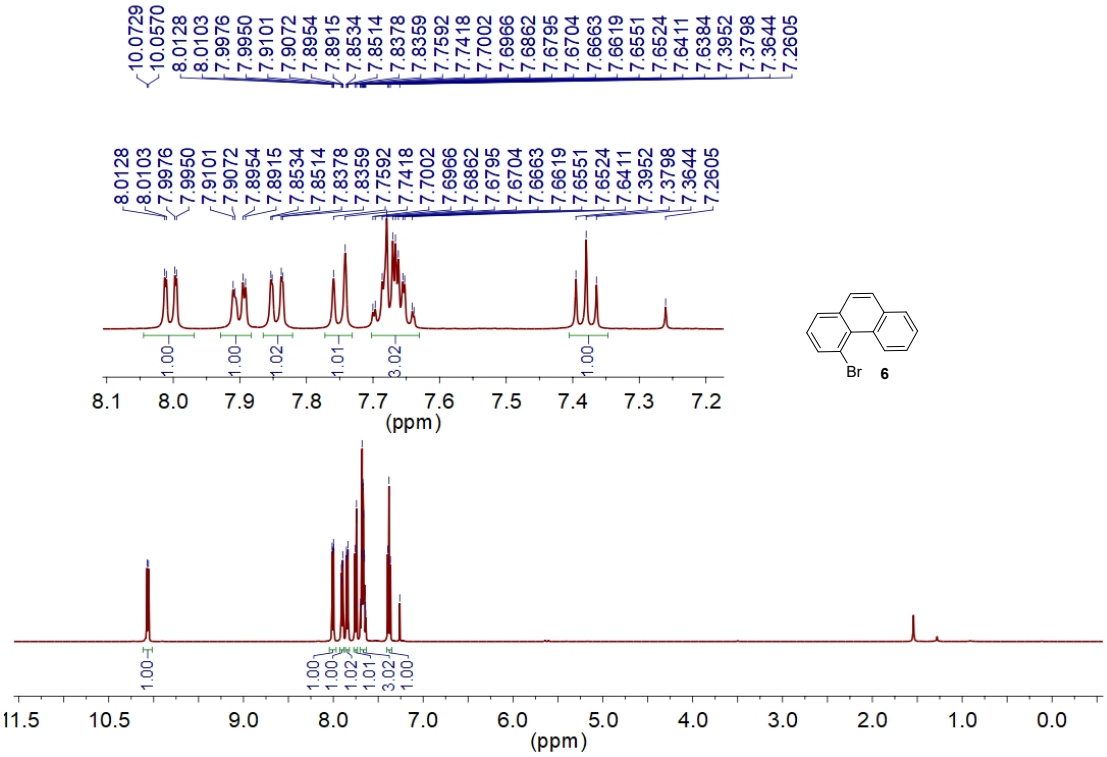

Figure S25. ^{1}H NMR (500 MHz) spectra of **6** recorded in $CDCl_3$ at room temperature.

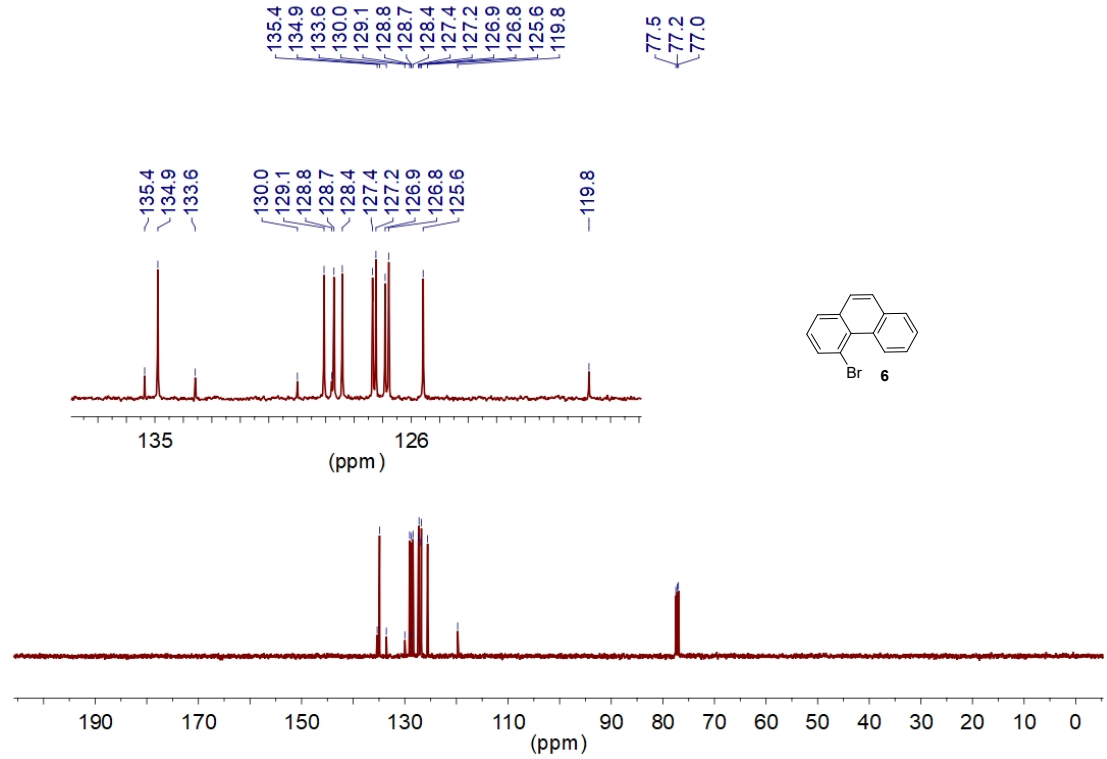

Figure S26. ^{13}C NMR (125 MHz) spectra of **6** recorded in $CDCl_3$ at room temperature.

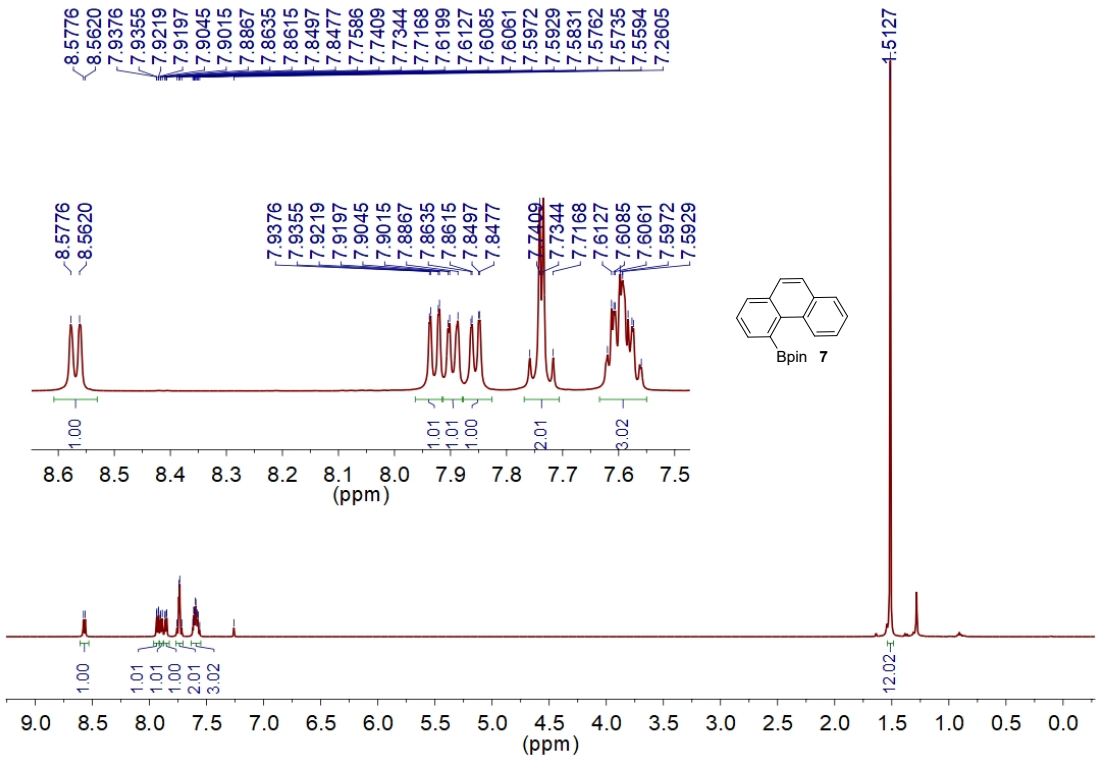

Figure S27. ^{1}H NMR (500 MHz) spectra of **7** recorded in $CDCl_3$ at room temperature.

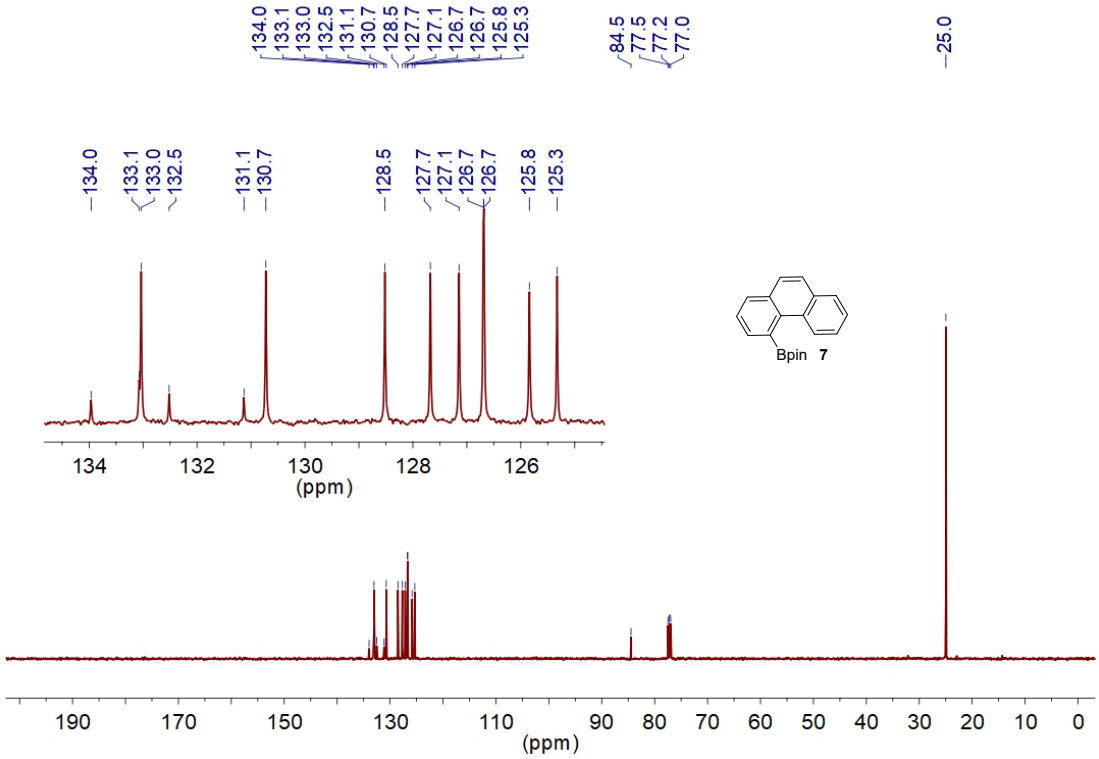

Figure S28. ^{13}C NMR (125 MHz) spectra of **7** recorded in $CDCl_3$ at room temperature.

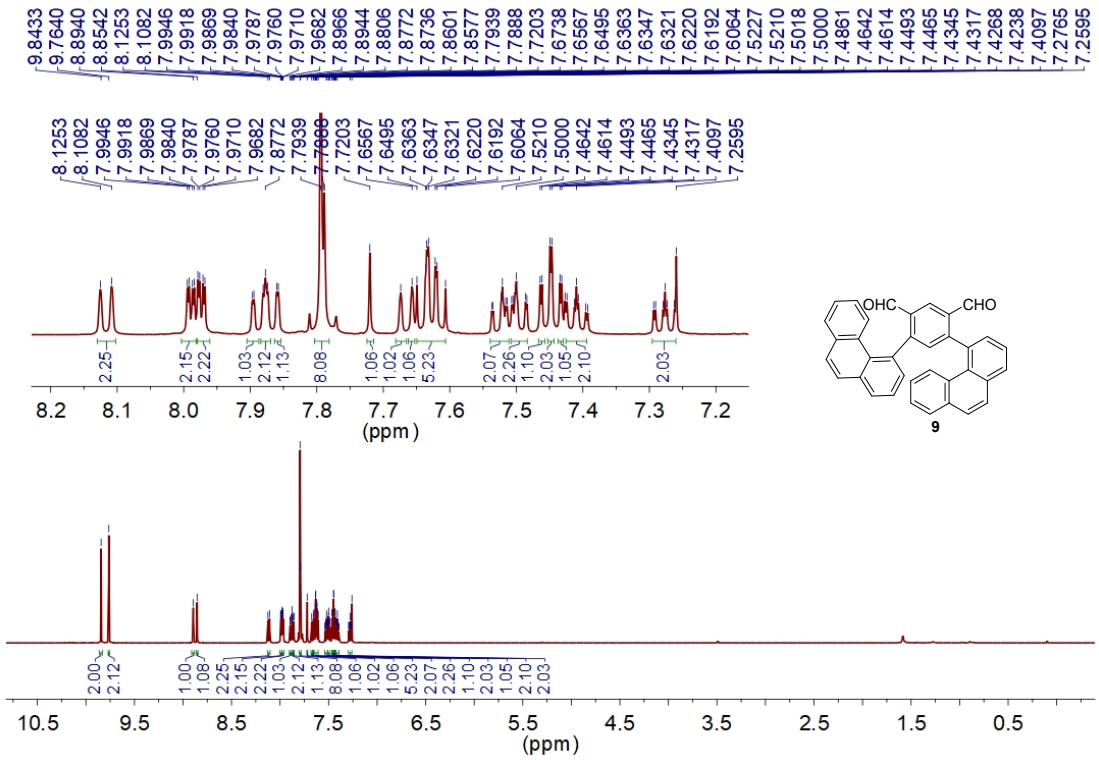

Figure S29. ^{1}H NMR (500 MHz) spectra of **9** recorded in $CDCl_3$ at room temperature.

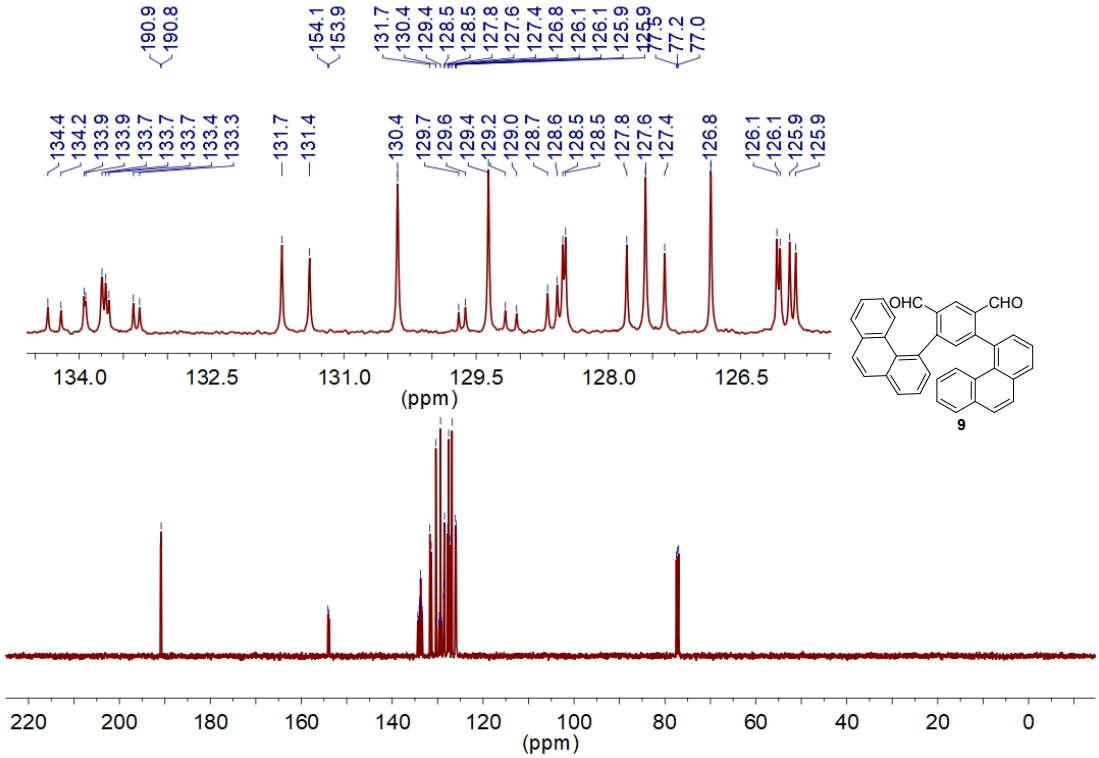

Figure S30. ^{13}C NMR (125 MHz) spectra of **9** recorded in $CDCl_3$ at room temperature.

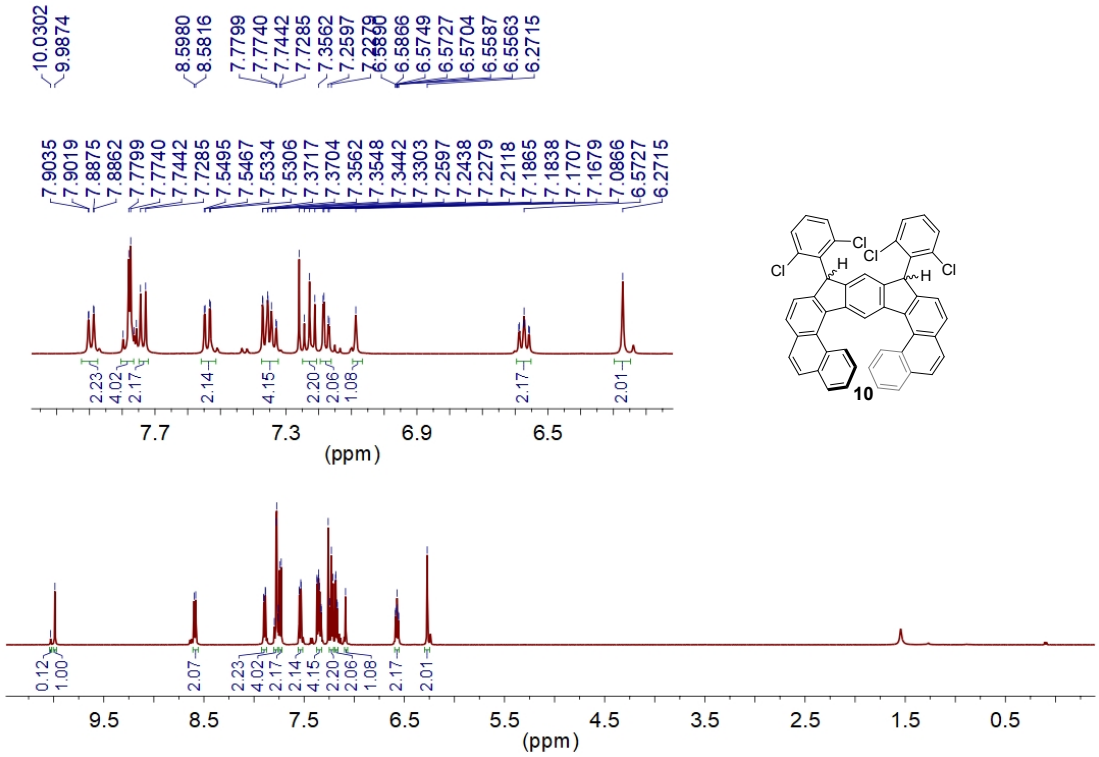

Figure S31. ^{1}H NMR (500 MHz) spectra of **10** recorded in $CDCl_3$ at room temperature.

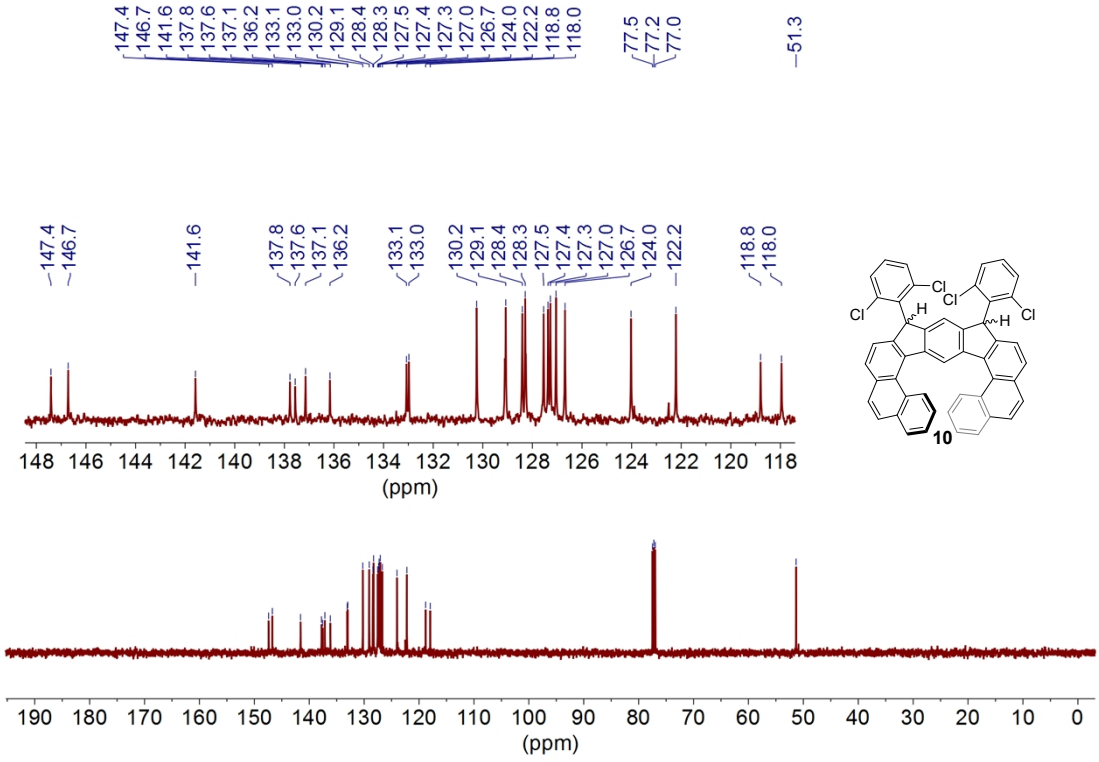

Figure S32. ^{13}C NMR (500 MHz) spectra of **10** recorded in $CDCl_3$ at room temperature.

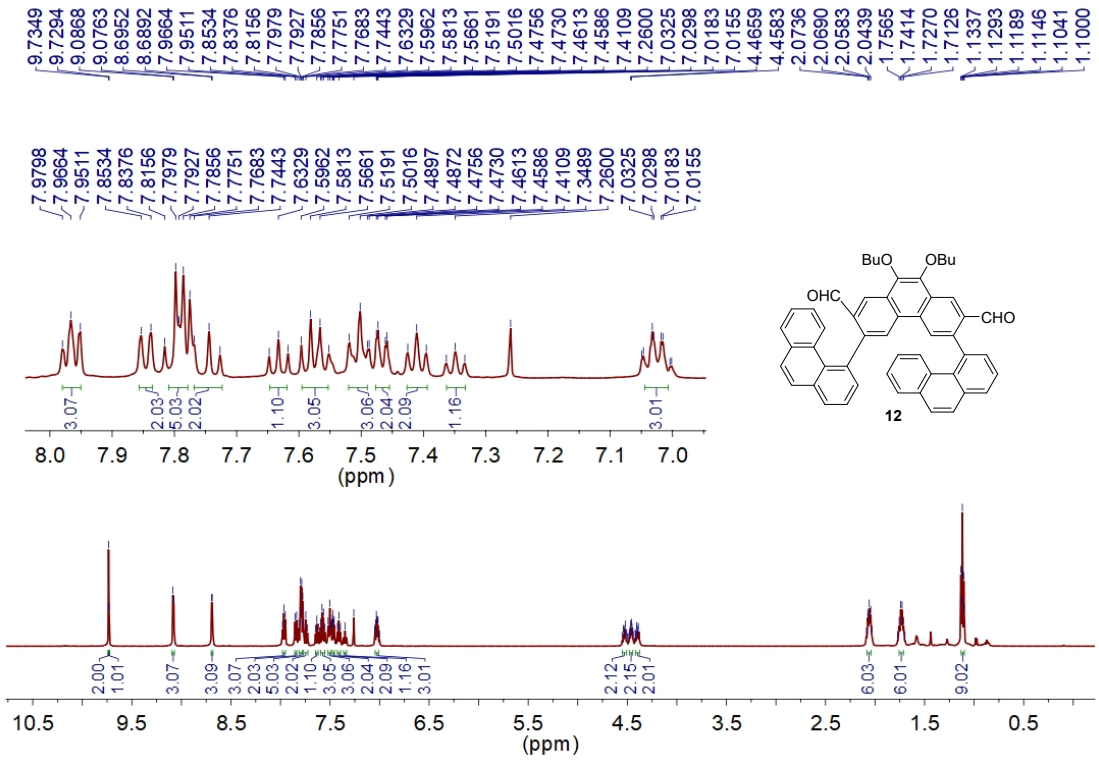

Figure S33. ^{1}H NMR (500 MHz) spectra of **12** recorded in $CDCl_3$ at room temperature.

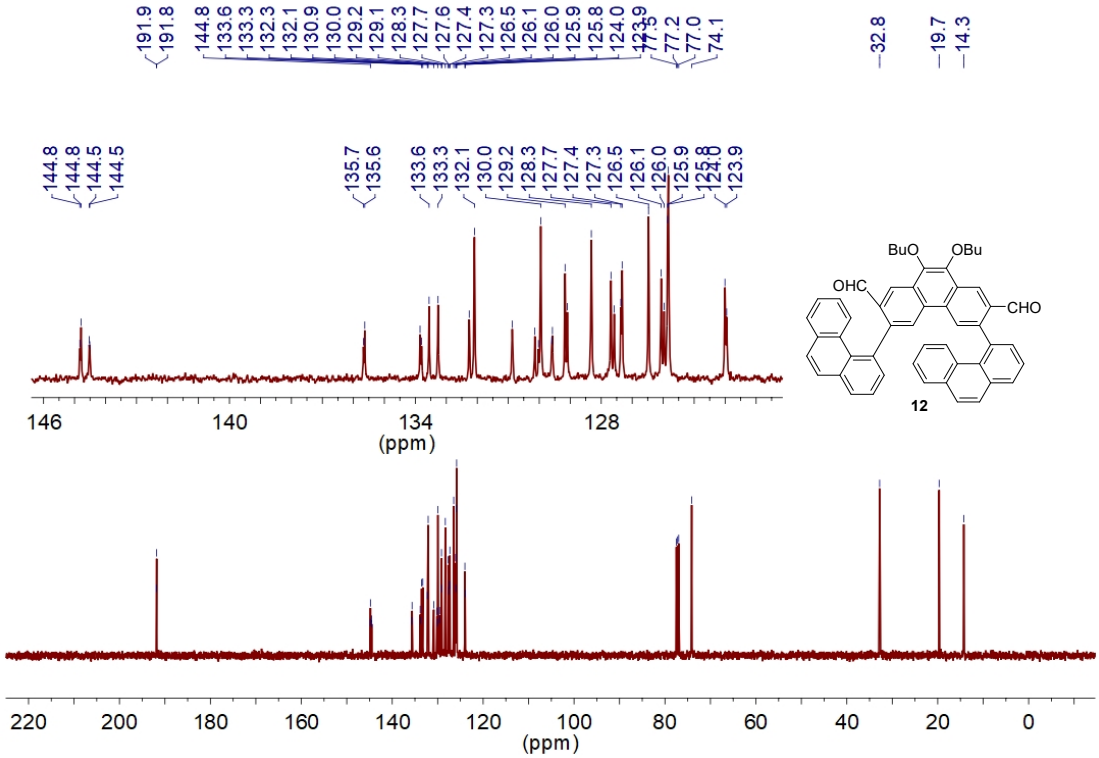

Figure S34. ^{13}C NMR (125 MHz) spectra of **12** recorded in $CDCl_3$ at room temperature.

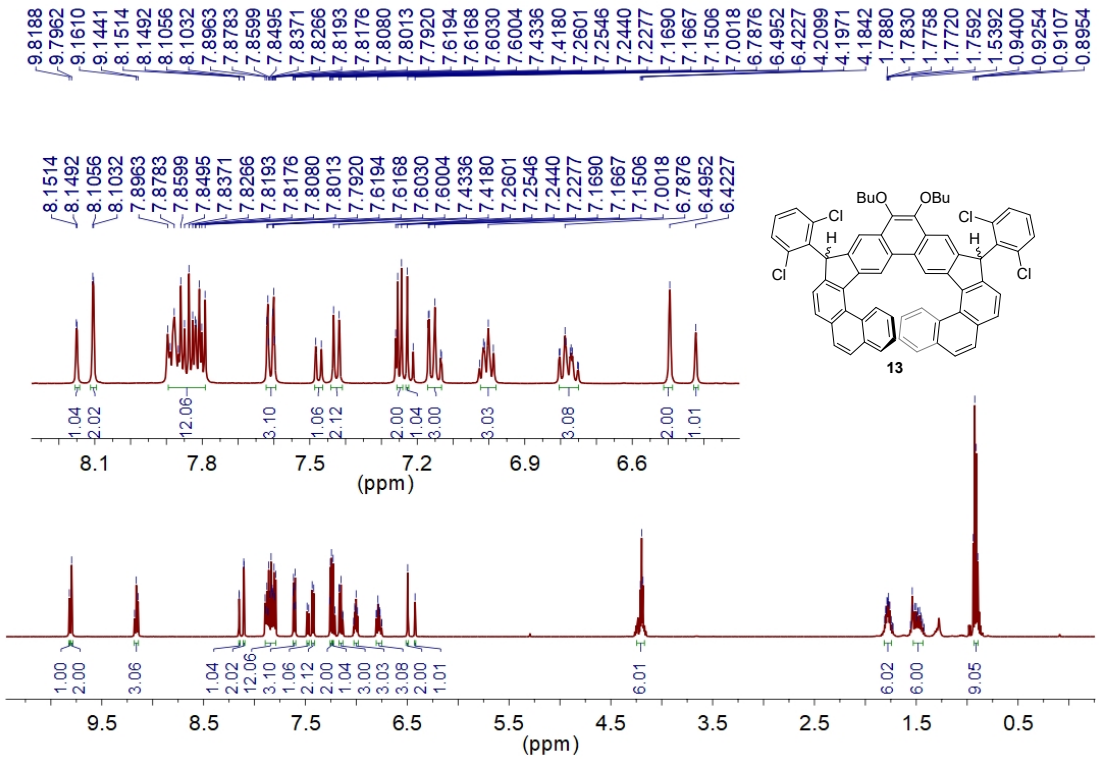

Figure S35. ^{1}H NMR (500 MHz) spectra of **13** recorded in $CDCl_3$ at room temperature.

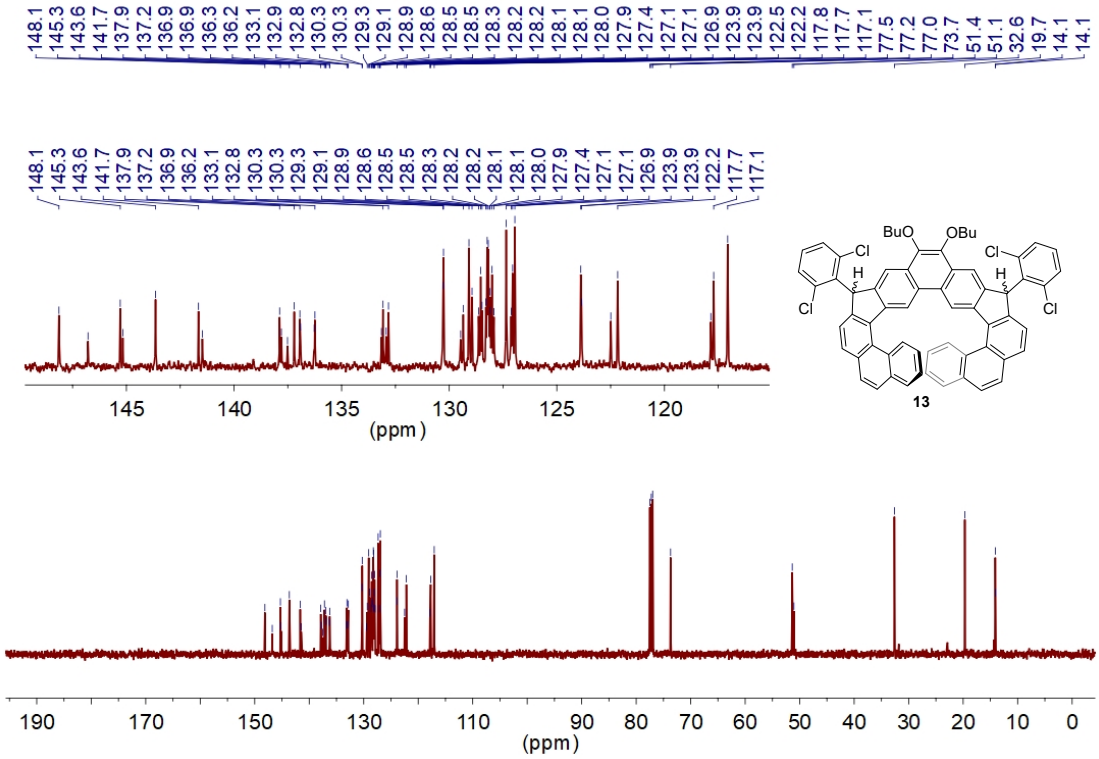

Figure S36. ^{13}C NMR (125 MHz) spectra of **13** recorded in $CDCl_3$ at room temperature.

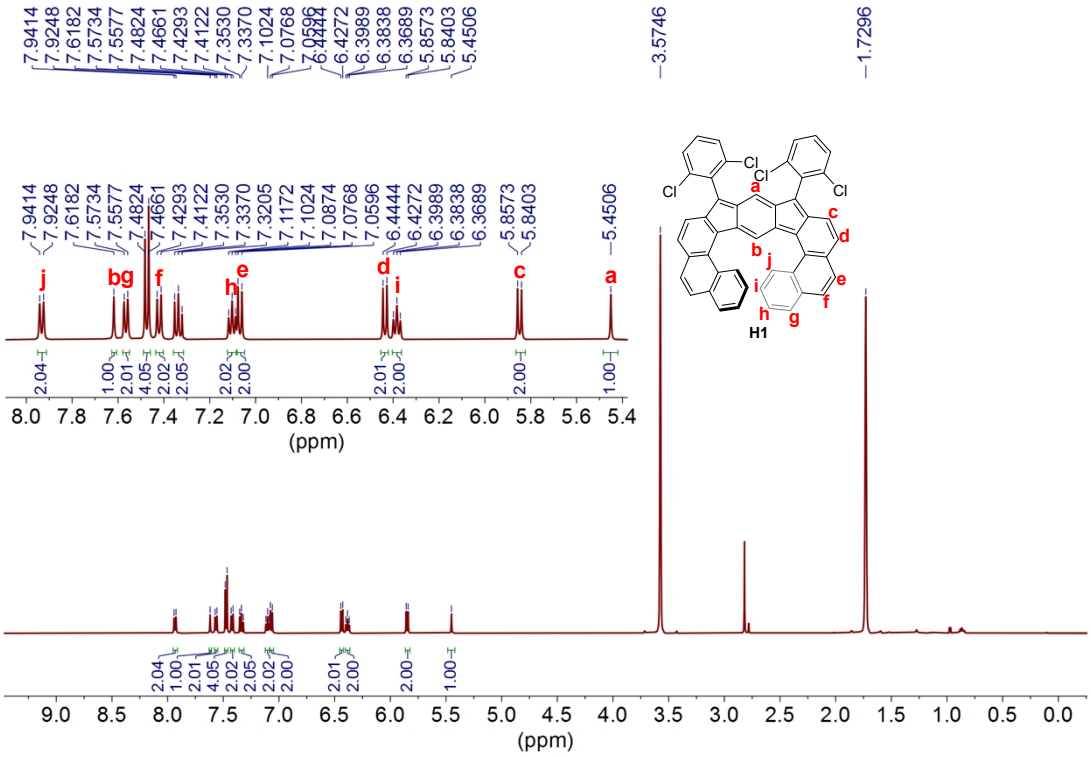

Figure S37. ^{1}H NMR (500 MHz) spectra of **H1** recorded in THF-d_8 at -20 °C.

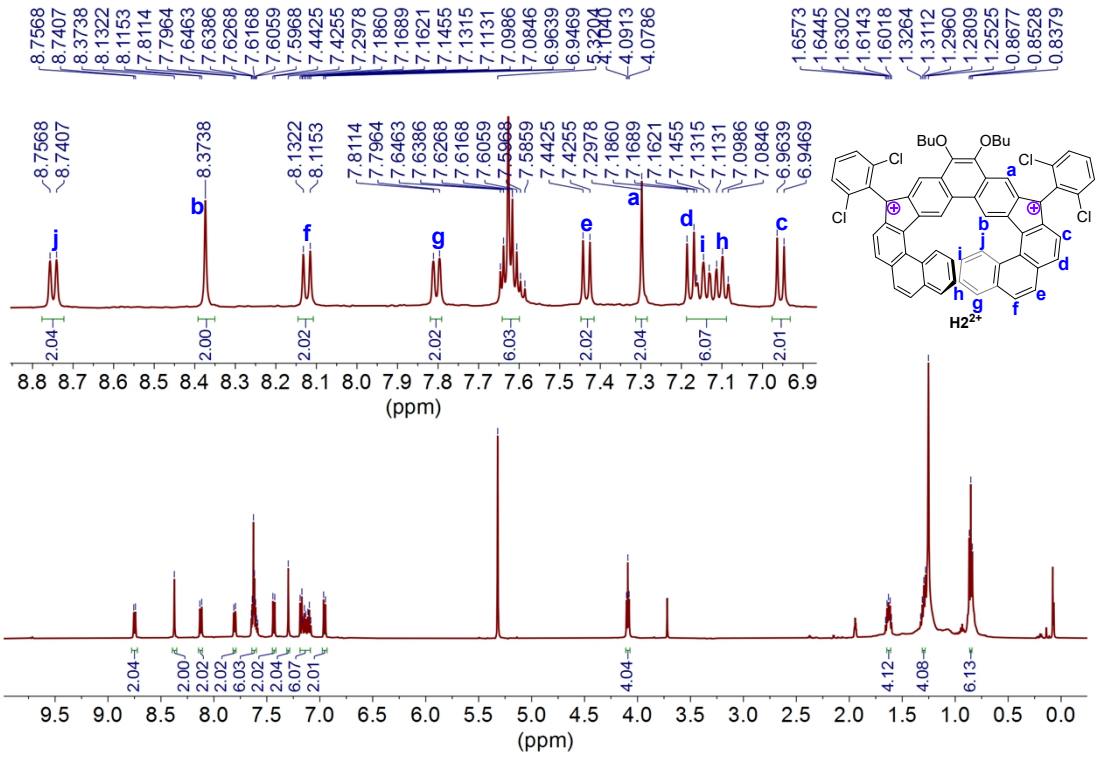

Figure S38. ^{1}H NMR (500 MHz) spectra of **H2**$^{2+}$ recorded in CD_2Cl_2 at room temperature.

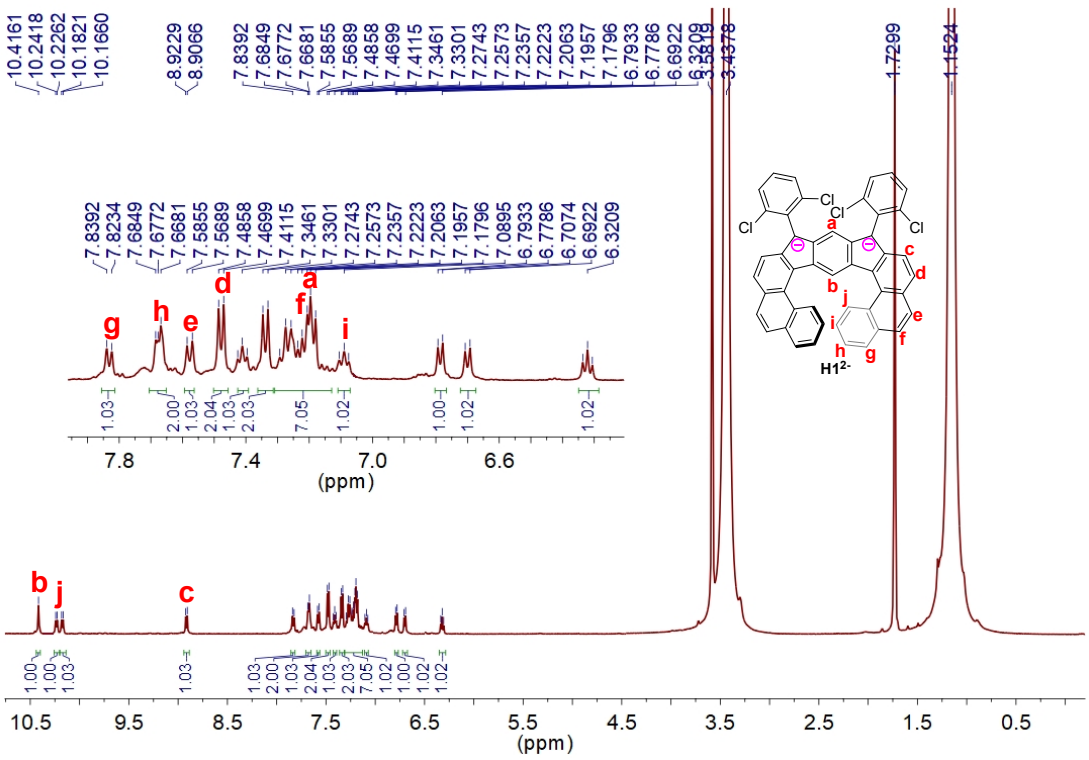

Figure S39. ^{1}H NMR (500 MHz) spectra of **H1^{2-}** recorded in THF-d_8 at room temperature.

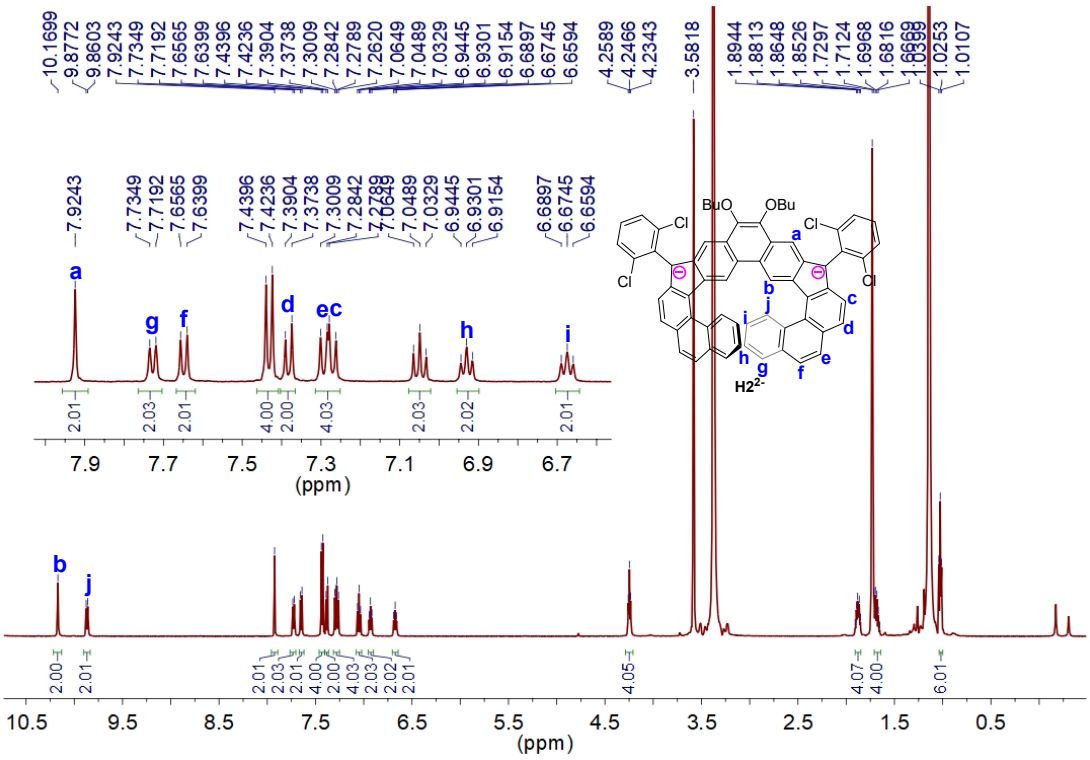

Figure S40. ^{1}H NMR (500 MHz) spectra of **H2^{2-}** recorded in THF-d_8 at room temperature.

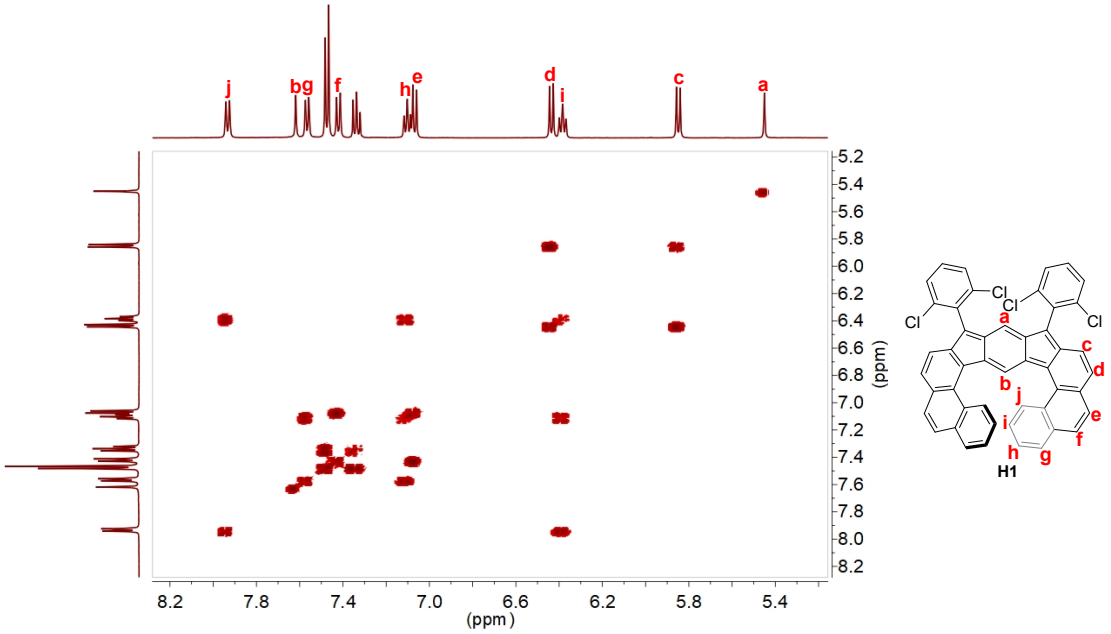

Figure S41. 2D COSY NMR (500 MHz) spectrum of **H1** in THF-d_8 at -20 °C.

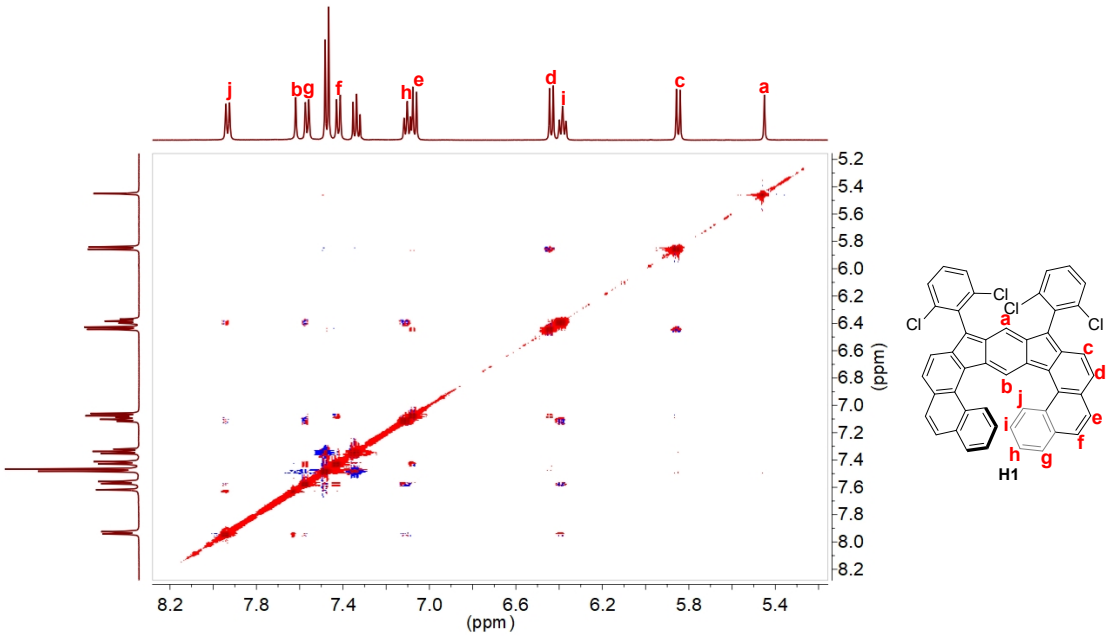

Figure S42. 2D NOESY NMR (500 MHz) spectrum of **H1** in THF-d_8 at -20 °C.

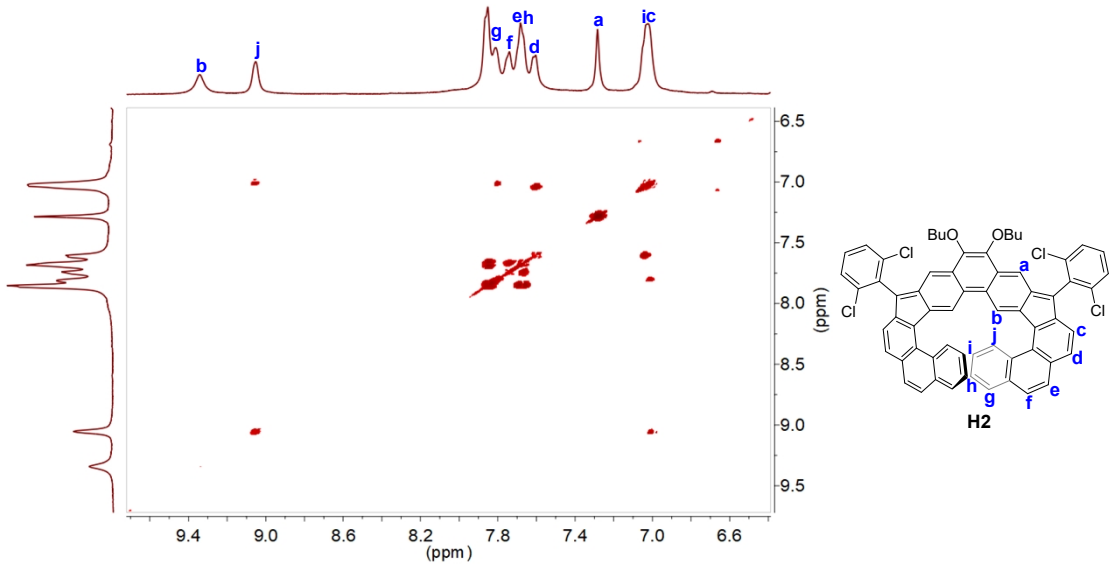

Figure S43. 2D COSY NMR (500 MHz) spectrum of **H2** in THF-d_8 at -100 °C.

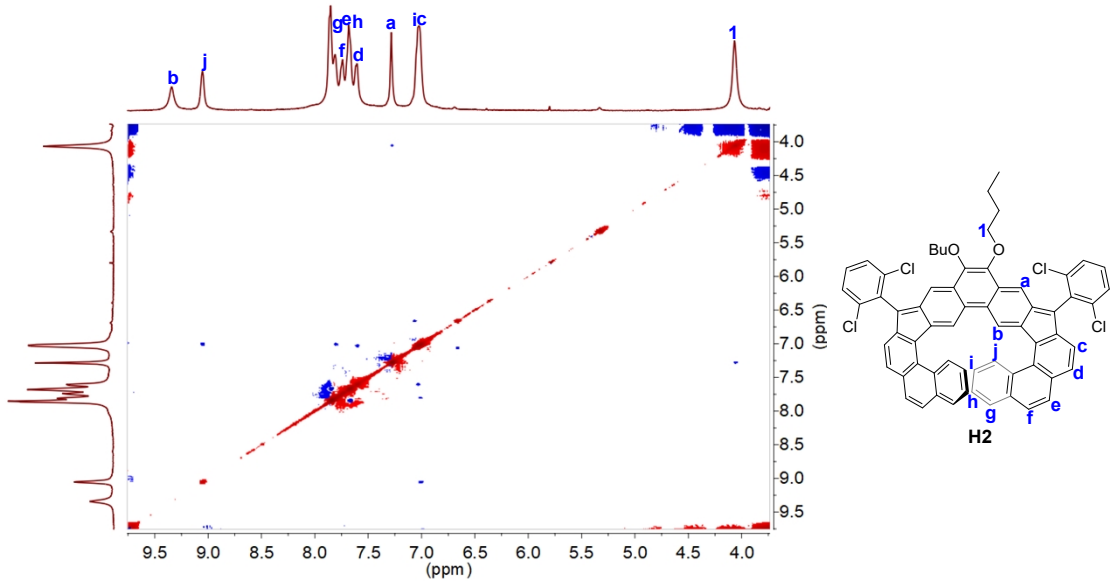

Figure S44. 2D R0ESY NMR (500 MHz) spectrum of **H2** in THF-d_8 at -100 °C.

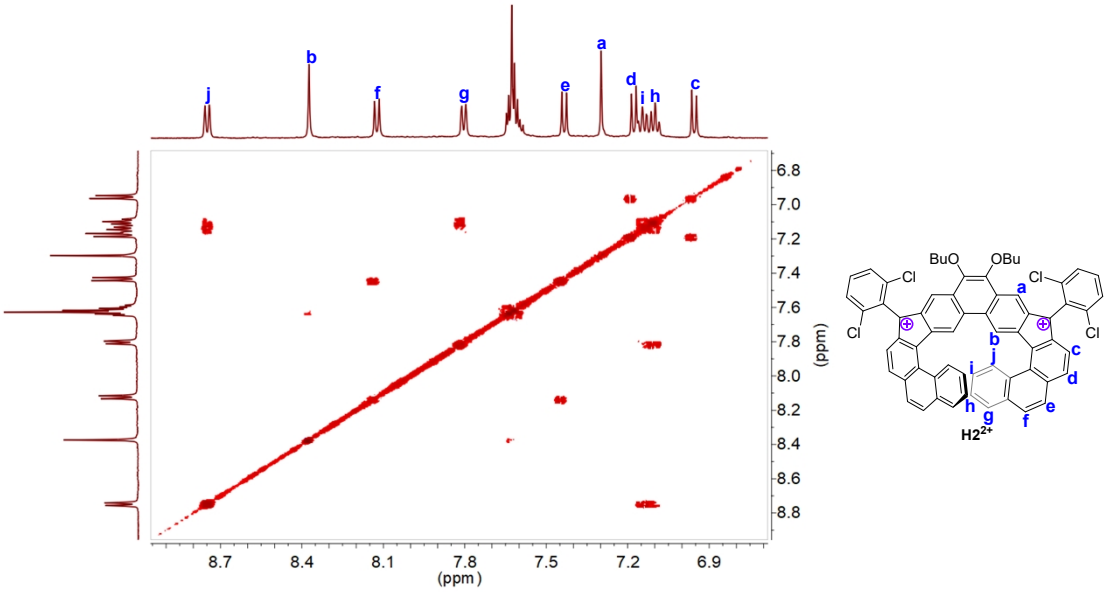

Figure S45. 2D COSY NMR (500 MHz) spectrum of **H2**$^{2+}$ in CD_2Cl_2 at room temperature.

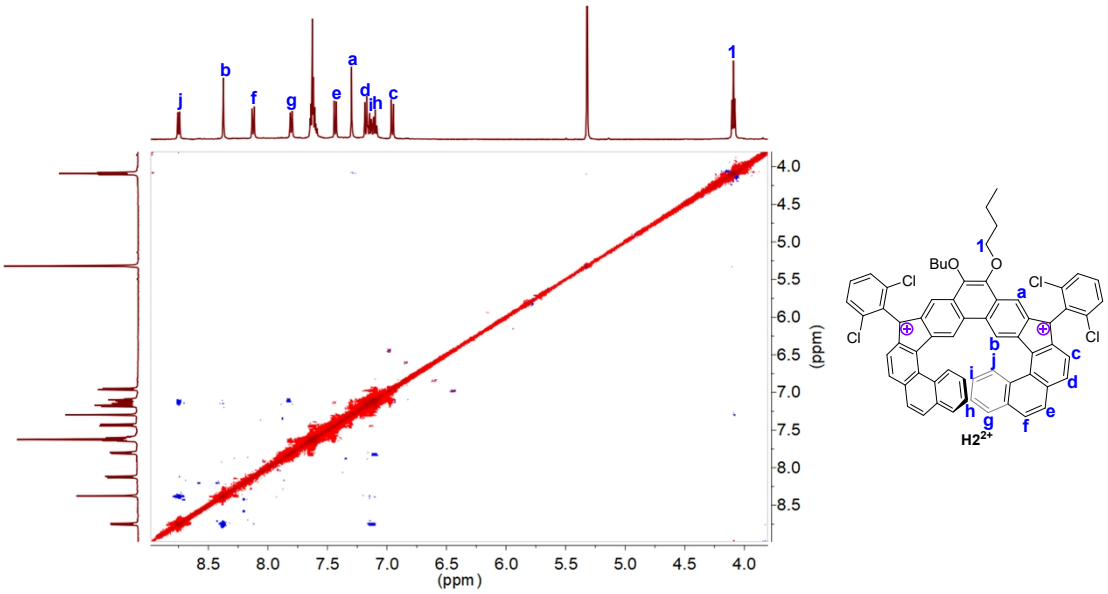

Figure S46. 2D ROESY NMR (500 MHz) spectrum of **H2**$^{2+}$ in CD_2Cl_2 at room temperature.

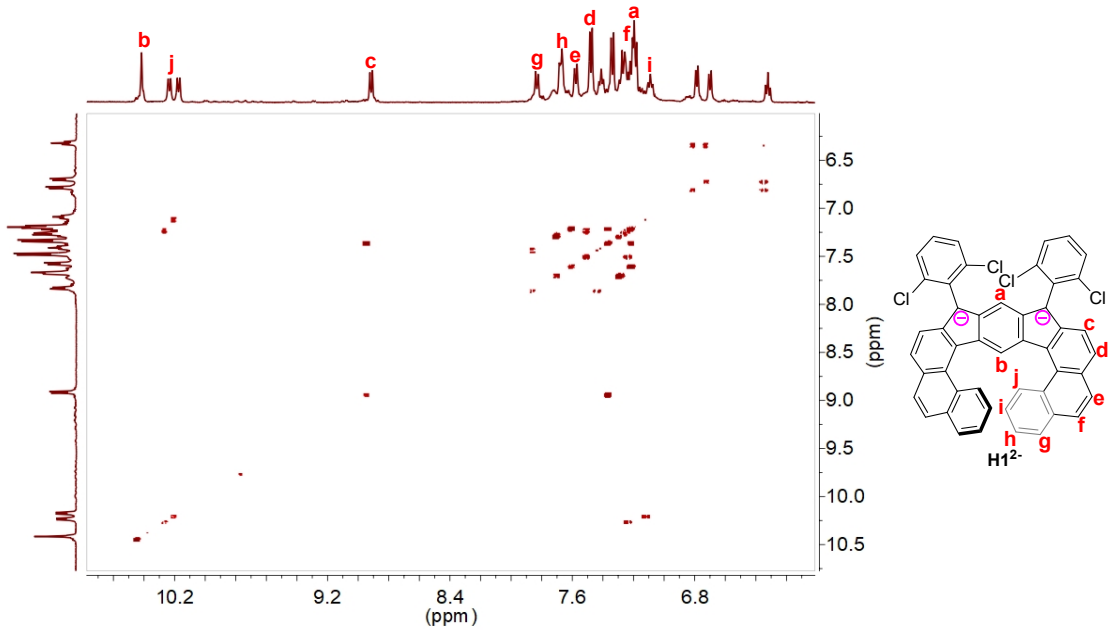

Figure S47. 2D COSY NMR (500 MHz) spectrum of **H1**$^{2-}$ in THF-d_8 at room temperature.

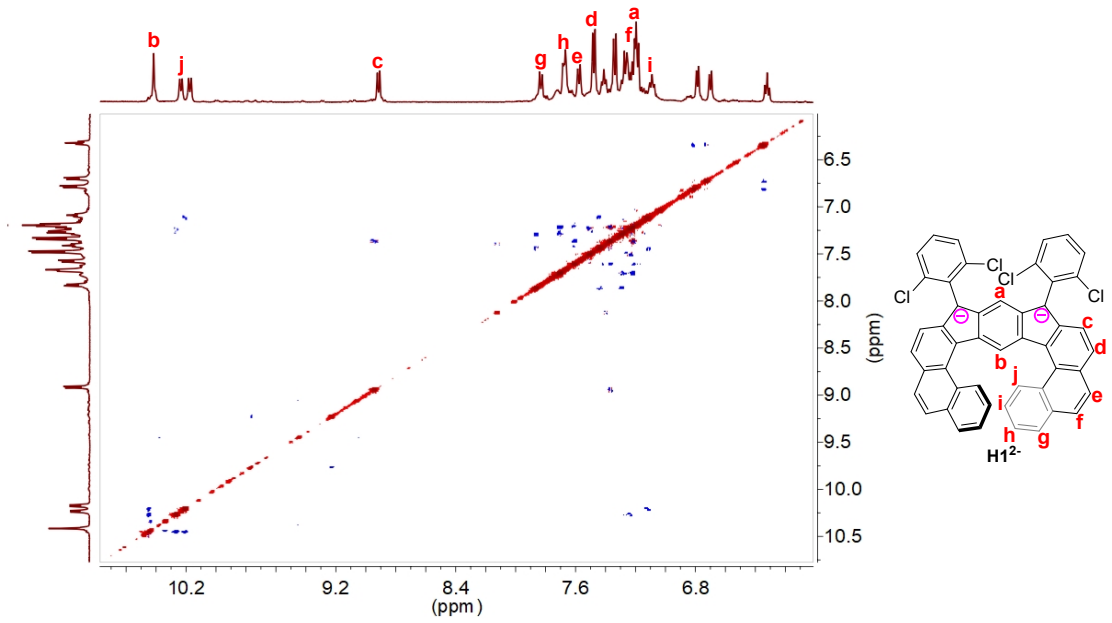

Figure S48. 2D ROESY NMR (500 MHz) spectrum of **H1**$^{2-}$ in THF-d_8 at room temperature.

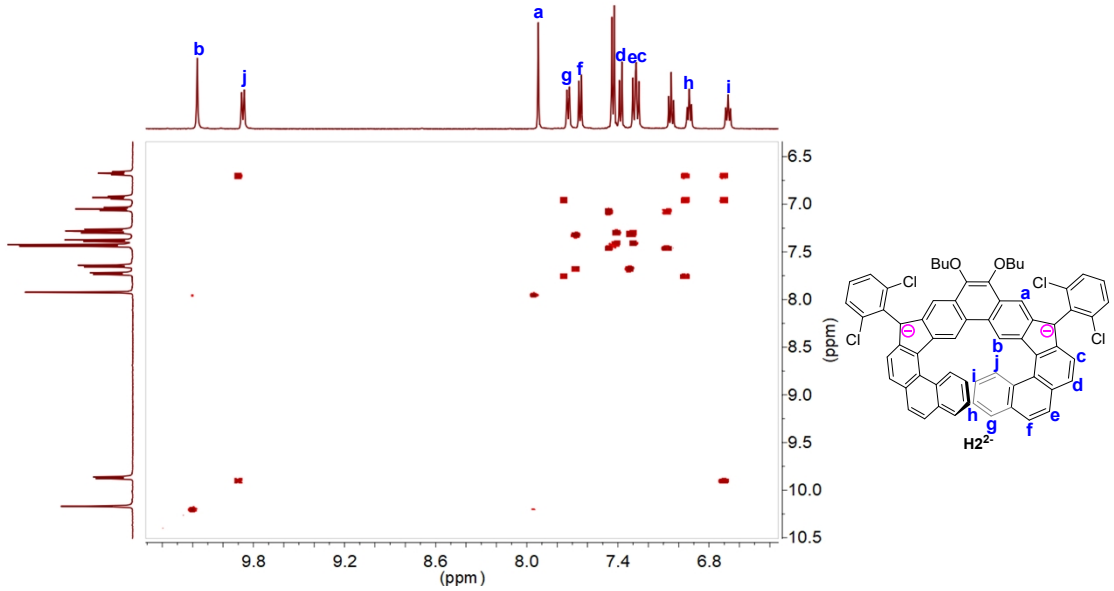

Figure S49. 2D COSY NMR (500 MHz) spectrum of **H2**$^{2-}$ in THF-d_8 at room temperature.

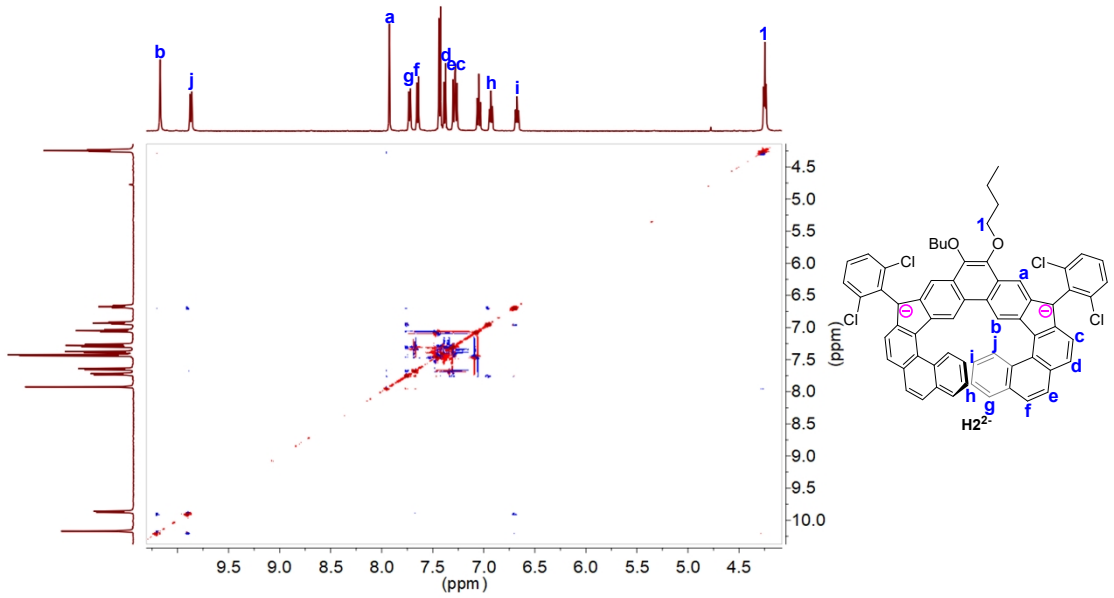

Figure S50. 2D ROESY NMR (500 MHz) spectrum of **H2**$^{2-}$ in THF-d_8 at room temperature.

6. References

(1) F. P. Gasparro, N. H. Kolodny, J. Chem. Educ. 1977, 54, 258.

(2) *Gaussian 09; Revision D.01*; M. J. Frisch, G. W. Trucks, H. B. Schlegel, G. E. Scuseria, M. A. Robb, J. R. Cheeseman, G. Scalmani, V. Barone, B. Mennucci, G. A. Petersson, H. Nakatsuji, M. Caricato, X. Li, H. P. Hratchian, A. F. Izmaylov, J. Bloino, G. Zheng, J. L. Sonnenberg, M. Hada, M. Ehara, K. Toyota, R. Fukuda, J. Hasegawa, M. Ishida, T. Nakajima, Y. Honda, O. Kitao, H. Nakai, T. Vreven, J. A. Montgomery, Jr., J. E. Peralta, F. Ogliaro, M. Bearpark, J. J. Heyd, E. Brothers, K. N. Kudin, V. N. Staroverov, R. Kobayashi, J. Normand, K. Raghavachari, A. Rendell, J. C. Burant, S. S. Iyengar, J. Tomasi, M. Cossi, N. Rega, J. M. Millam, M. Klene, J. E. Knox, J. B. Cross, V. Bakken, C. Adamo, J. Jaramillo, R. Gomperts, R. E. Stratmann, O. Yazyev, A. J. Austin, R. Cammi, C. Pomelli, J. W. Ochterski, R. L. Martin, K. Morokuma, V. G. Zakrzewski, G. A. Voth, P. Salvador, J. J. Dannenberg, S. Dapprich, A. D. Daniels, Ö. Farkas, J. B. Foresman, J. V. Ortiz, J. Cioslowski, and D. J. Fox, Gaussian, Inc., Wallingford CT, **2009**.

(3) (a) A. D. Becke, *J. Chem. Phys.* **1993**, *98*, 5648. (b) C. Lee, W. Yang, R. G. Parr, *Phys. Rev. B: Condens. Matter* **1988**, *37*, 785. (c) T. Yanai, D. Tew, N. Handy, *Chem. Phys. Lett.* **2004**, *393*, 51. (d) R. Ditchfield, W. J. Hehre, J. A. Pople, *J. Chem. Phys.* **1971**, *54*, 724. (e) W. J. Hehre, R. Ditchfield, J. A. Pople, *J. Chem. Phys.* **1972**, *56*, 2257. (f) P. C. Hariharan, J. A. Pople, *Theor. Chim. Acta* **1973**, *28*, 213.

(4) (a) S. Yamanaka, M. Okumura, M. Nakano and K. Yamaguchi, *J. Mol. Struct.* **1994**, *310*, 205. (b) K. Kamada, K. Ohta, A. Shimizu, T. Kubo, R. Kishi, H. Takahashi, E. Botek, B. Champagne and M. Nakano, *J. Phys. Chem. Lett.* **2010**, *1*, 937. (c) Z. Chen, C. S. Wannere, C. Corminboeuf, R. Puchta, P. v. R. Schleyer, *Chem. Rev.* **2015**, *105*, 3842.

(5) (a) D. Geuenich, K. Hess, F. Köhler, R. Herges, *Chem. Rev.* **2005**, 105, 3758. (b) H. Fallah-Bagher-Shaidaei, S. S. Wannere, C. Corminboeuf, R., Puchta, P. v. R. Schleyer, *Org. Lett.* **2006**, *8*, 863.

(6) (a) C. Gonzalez, H. B. Schlegel, *J. Chem. Phys.* **1989**, 90, 2154. (b) C. Gonzalez, H. B. Schlegel, *J. Phys. Chem.* **1990**, 94, 5523.